J. Phycol. **50,** 81–100 (2014)

DOI: 10.1111/jpy.12134

PHYLOGENETIC RELATIONSHIPS, MORPHOLOGICAL VARIATION, AND TOXIN PATTERNS IN THE *ALEXANDRIUM OSTENFELDII* (DINOPHYCEAE) COMPLEX: IMPLICATIONS FOR SPECIES BOUNDARIES AND IDENTITIES[1]

Anke Kremp[2]

Finnish Environment Institute, Marine Research Centre, Erik Palménin aukio 1, Helsinki 00560, Finland

Pia Tahvanainen

Finnish Environment Institute, Marine Research Centre, Erik Palménin aukio 1, Helsinki 00560, Finland
University of Helsinki, Tvärminne Zoological Station, J.A. Palménin tie 260, Hanko 10900, Finland

Wayne Litaker

National Oceanic and Atmospheric Administration, National Ocean Service, Center for Coastal Fisheries and Habitat Research, 101 Pivers Island Rd., Beaufort North Carolina

Bernd Krock

Alfred Wegener Institute for Polar and Marine Research, Division of Biosciences, Am Handelshafen 12, Bremerhaven 27570, Germany

Sanna Suikkanen

Finnish Environment Institute, Marine Research Centre, Erik Palménin aukio 1, Helsinki 00560, Finland

Chui Pin Leaw

Institute of Biodiversity and Environmental Conservation, University Malaysia Sarawak, Kota Samarahan Sarawak,, 94300, Malaysia

and Carmelo Tomas

University of North Carolina at Wilmington, Center for Marine Science, Myrtle Grove 2336, Wilmington, North Carolina

Alexandrium ostenfeldii **(Paulsen) Balech and Tangen and *A. peruvianum* (Balech and B.R. Mendiola) Balech and Tangen are morphologically closely related dinoflagellates known to produce potent neurotoxins. Together with *Gonyaulax dimorpha* Biecheler, they constitute the *A. ostenfeldii* species complex. Due to the subtle differences in the morphological characters used to differentiate these species, unambiguous species identification has proven problematic. To better understand the species boundaries within the *A. ostenfeldii* complex we compared rDNA data, morphometric characters and toxin profiles of multiple cultured isolates from different geographic regions. Phylogenetic analysis of rDNA sequences from cultures characterized as *A. ostenfeldii* or *A. peruvianum* formed a monophyletic clade consisting of six distinct groups. Each group examined contained strains morphologically identified as either *A. ostenfeldii* or *A. peruvianum*. Though key morphological characters were generally found to be highly variable and not consistently distributed, selected plate features and toxin profiles differed significantly among phylogenetic clusters. Additional sequence analyses revealed a lack of compensatory base changes in ITS2 rRNA structure, low to intermediate ITS/5.8S uncorrected genetic distances, and evidence of reticulation. Together these data (criteria currently used for species delineation in dinoflagellates) imply that the *A. ostenfeldii* complex should be regarded a single genetically structured species until more material and alternative criteria for species delimitation are available. Consequently, we propose that *A. peruvianum* is a heterotypic synonym of *A. ostenfeldii* and this taxon name should be discontinued.**

Key index words: ***Alexandrium ostenfeldii*****;** ***Alexandrium peruvianum*****; ITS2 compensatory base changes; morphology; Paralytic Shellfish Toxins; phylogeny; spirolides**

Abbreviations**: AIC, Akaike Information Criterion; BI, Bayesian inference; BIC, Bayesian Information Criterion; HAB, harmful algal bloom; ML, maximum likelihood; PSP, paralytic shellfish poisoning**

[1]Received 15 February 2013. Accepted 3 September 2013.
[2]Author for correspondence: e-mail anke.kremp@ymparisto.fi.
Editorial Responsibility: O. De Clerck (Associate Editor)

Many of the global harmful algal blooms (HABs) are caused by the genus *Alexandrium*. A number of species belonging to this genus produce neurotoxic paralytic shellfish poisoning (PSP) toxins (Anderson et al. 2012) that can severely affect human health and marine biota (Wang 2008). PSP toxins account for the majority of harmful events caused by *Alexandrium*, however other toxin families, such as spirolides, goniodomins, and gymnodimines (Cembella et al. 2000, Hsia et al. 2006, Van Wagoner et al. 2011) have been detected in some species of the genus and may sometimes occur together in one species or strain (Tomas et al. 2012). *Alexandrium* species are often globally distributed, occurring in a variety of habitats and spanning all geographic zones (Taylor et al. 1995, Lilly et al. 2007, McCauley et al. 2009). The successful colonization and persistence of *Alexandrium* in diverse environments have been attributed to advantageous ecophysiological adaptations that many members of the genus possess (Anderson et al. 2012).

Within the genus, Balech (1995) classified species that were morphologically distinct, but clearly related, into groups. Molecular trees, showing that the species of the respective groups typically cluster together, generally support such relationships (Scholin et al. 1994, John et al. 2003, Leaw et al. 2005, Orr et al. 2011). However, morphological delineations within the complexes are not always confirmed by molecular data (Hansen et al. 2003, Lilly et al. 2005, 2007, Penna et al. 2005) suggesting that original taxonomic distinction of the species in the complexes may not reflect evolutionary relationships.

One of the groups defined by Balech is the *A. ostenfeldii* group (Balech 1995), a globally distributed complex of species known to produce several different potent phycotoxins: PSTs, spirolides, and gymnodimines (Hansen et al. 1992, Cembella et al. 2000, Van Wagoner et al. 2011). Based on their similar morphology, Balech (1995) considered three formally described species, *A. ostenfeldii* (Paulsen) Balech and Tangen (Paulsen 1904, Balech and Tangen 1985), *A. peruvianum* (Balech and B.R. Mendiola) Balech and Tangen (Balech and de Mendiola 1977, Balech and Tangen 1985) and *Gonyaulax dimorpha* Biecheler (Biecheler 1952) to be closely related. All are characterized by large globe shaped cells covered by thin walled thecae that easily collapse. Most importantly, they share a narrow, conspicuously asymmetrical first apical plate exhibiting a definite large ventral pore with varying dimensions.

Alexandrium ostenfeldii and *A. peruvianum* are formally delineated by differences in cell shape and features of the first apical (1′), sulcal anterior (s.a.) and sixth precingular (6″) plates that were detected in the type material from Oslofjord, Norway and Callao, Peru, respectively (Balech and de Mendiola 1977, Balech and Tangen 1985). *Alexandrium ostenfeldii* cells are generally considered to be larger, and longer than wide, while *A. peruvianum* cells appear smaller and slightly wider than long. The straight (or sometimes irregular) anterior and posterior right margins of the narrow 1′ plate of *A. ostenfeldii* (Paulsen 1904) form a distinct angle around a large ventral pore, whereas in *A. peruvianum* the right anterior margin of this plate is typically curved, and the enclosed pore is smaller (Balech and de Mendiola 1977). The s.a. plate in *A. ostenfeldii* is generally low and wide with a horizontal anterior margin and a slightly oblique right end that makes it appear like a door-latch. In *A. peruvianum,* this plate is A-shaped or triangular. The 6″ plate is also typically wider in *A. ostenfeldii* compared to *A. peruvianum*. *G. dimorpha* was described from material collected in a coastal Mediterranean lagoon of Southern France (Biecheler 1952) and appears distinct from the former two species by a conspicuously wide and anteriorly extended 1′ plate and a horseshoe-shaped s.a. plate that penetrates into the epitheca. Given that the identity of the latter species has not been accepted by some authors (Balech 1995), and examination of the type material was not possible, this species has never been formally transferred to the genus *Alexandrium*.

Although morphological differences among *A. ostenfeldii* and *A. peruvianum*, were well defined in the material originally investigated, further studies on samples from other locations revealed that distinctive plate characters vary considerably among and within geographic populations and even within strains (Balech 1995, MacKenzie et al. 1996, Cembella et al. 2000, Lim et al. 2005, Kremp et al. 2009). Given this extensive morphological variation, recent *A. ostenfeldii* and *A. peruvianum* identifications have been made with reservations, and scientists repeatedly emphasized the necessity to re-assess the validity of distinctive characters (Lim et al. 2005, Kremp et al. 2009). Consistent assignment has furthermore been complicated by the lack of consensus regarding the weight of the different diagnostic features: while some investigators have given priority to the s.a. shape (Bravo et al. 2006, Tomas et al. 2012), others considered the anterior 1′ margin most important (MacKenzie et al. 1996, Kremp et al. 2009). In addition to these inconsistencies, morphogenetic identification is not simple either, despite the availability of extensive sequence data and recognition of specific genetic signatures (Touzet et al. 2011). GenBank contains numerous identical sequences from isolates assigned to *A. ostenfeldii* and *A. peruvianum*.

The need for clear identification guidelines and a better taxonomic understanding of the *A. ostenfeldii* group is becoming more and more evident, since blooms of the respective species have increased significantly in the past decades. Both *A. ostenfeldii* and *A. peruvianum* are now regularly encountered in field surveys and monitoring programs worldwide (MacKenzie et al. 2004, Gribble et al. 2005, Nagai et al. 2010, Brown et al. 2010, Touzet et al. 2011). Dense blooms associated with toxins have been

reported from Peru (Sanchez et al. 2004), the estuaries of the U.S. east coast (Borkman et al. 2012, Tomas et al. 2012) and the Baltic Sea (Witek 2004, Hakanen et al. 2012).

Species delimitations in dinoflagellate groups with ambiguous morphological differentiation, such as the genus *Alexandrium*, have generally been challenging. Phylogenetic criteria have been proposed to assess species boundaries among closely related taxa, such as the level of sequence divergence (Litaker et al. 2007), and presence/absence of intragenomic polymorphisms (Miranda et al. 2012). The "biological species concept" (Mayr 1942), which defines a species based on the ability to interbreed, has been taken into account in a few studies (Brosnahan et al. 2010). Though powerful, this latter approach is difficult to document in culture. For many years, it was assumed that formation of reproductive cysts was a reliable indicator of sexual compatibility (Pfiester and Anderson 1987). It is now known that sexuality and outbreeding cannot always be inferred from the presence of cysts because reproduction processes are far more complex and versatile than previously suspected (Kremp 2013). Recently, an alternative method for examining reproductive isolation has been applied to dinoflagellates (Leaw et al. 2010). That method predicts sexual compatibility or reproductive isolation in eukaryotes-based compensatory base changes (CBCs) in transcripts of the ITS2 rDNA region (Coleman 2009). The need for integrating these different lines of evidence into existing morphological species delimitations to more accurately identify species boundaries among closely related lineages has been emphasized by both systematic biologists (de Queiroz 2007) and protistologists (Boenigk et al. 2012).

This study compares rDNA data, morphometric characters and toxin profiles of a large set of representative *A. ostenfeldii* and *A. peruvianum* isolates from different geographic regions. Our aim was 2-fold: (i) to determine how consistently phylogenetic analysis of rDNA sequence data, diagnostic morphological characters, and physiological traits segregated into distinct groups consistent with the presently described morphospecies, and (ii) to ascertain whether there were more species in the *A. ostenfeldii* complex different from those previously described. The phylogenetic analysis including sequences obtained from GenBank as well as from *A. ostenfeldii* and *A. peruvianum* isolates sequenced in this study, revealed six distinct genetic subgroups. A sufficient number of representative cultures were available from groups 1, 2, 5, and 6 to evaluate group-wise variations in the morphological features originally used to describe *A. ostenfeldi* and *A. peruvianum* as well as their characteristic toxin profiles. The resulting phylogenetic, morphological, and toxicological analyses made it possible to re-evaluate the original species descriptions in the *A. ostenfeldii* complex.

MATERIAL AND METHODS

Isolates. The strains analyzed in this study (Table 1) represent most of the *A. ostenfeldii* and *A. peruvianum* isolates presently available in culture collections and research laboratories worldwide as well as a number of strains isolated specifically for this study. These isolates span different geographic regions ranging from the subarctic coast of Iceland to tropical South America where the two morphospecies have been recorded in the recent past. New monoclonal strains from the Baltic, Oslofjord/Norway, Iceland, and Canada were grown from cysts isolated from sediment samples as described in Tahvanainen et al. (2012). All cultures were maintained at 16°C, 50 µmol photons $\cdot$ m^{-2} $\cdot$ s^{-1} in f/2 without silica addition (Guillard and Ryther 1962) sterilized filtered local (Baltic) seawater with salinities adjusted to natural conditions of the original environment. Molecular, morphological, and/or toxin data were generated for 29 strains (Table 1). To complement the alignment, sequences of eight additional *A. ostenfeldii* strains (not included in morphological and toxin analyses) were obtained from Genbank together with sequences of the related species *A. minutum* and *A. insuetum*.

DNA extraction, PCR amplification, and sequencing. To determine the ITS through D1-D2 LSU rDNA sequences of the various isolates, cells were harvested from exponentially growing cultures and their DNA was extracted. To accomplish this, 15 mL of culture was centrifuged for 15 min at 21,000*g*. After aspiration of the supernatant, loose pellets were moved to 1.5 mL Eppendorf-tubes and re-centrifuged for 5 min at 21,000*g* in a microfuge. Cells of the resulting pellets were disrupted using a pestle (Pellet Pestle™; Kontes Glass Company Kimble, Vineland, NJ, USA). To avoid cross contamination, a new pestle was used for every sample. DNA extraction and subsequent purification were performed using a Plant Mini Kit (Qiagen, Hilden, the Netherlands). The resulting DNA was purified using the Template Purification Kit (Roche, Basel, Switzerland) according to the manufacturer's instructions.

PCR amplification of the purified genomic DNA samples was performed in 25 µL reaction volume using PCR beads (Illustra PuReTaq Ready-to-go-PCR-beads; GE Healthcare, Piscataway, NJ, USA). The reaction mix contained 22 µL of sterile MQ (Milli-Q; Millipore Corporation, Billerica, MA, USA) water, 1 µL of each primer (10 µM), and 1–2 µL of genomic DNA (~50 ng). The PCR amplification was carried out with a single denaturation step for 5 min at 95°C, followed by 30 cycles of 2 min at 95°C, 2 min at 54°C, and 4 min at 72°C, with the final extension for 7 min at 72°C. PCR products were purified using the GFX-PCR Purification Kit (Qiagen) following the manufacturer's protocol. DNA purity and concentration were measured with a NanoDrop ND-1000 spectrophotometer (Thermo Scientific, Waltham, MA, USA) and DNA samples were stored at −20°C until they were sequenced. For PCR amplification and sequencing of the ITS1/5.8S/-ITS2 and LSU D1/D2 regions, the forward and reverse primers of Adachi et al. (1994) and Scholin et al. (1994) were used. Each of the purified amplicons was directly sequenced in both directions on either an Applied Biosystems ABI3130XL Genetic Analyzer (16-capillaries) or ABI3730 DNA Analyzer (48-capillaries; Applied Biosystems, Carlsbad, CA, USA). For both instruments, the Applied Biosystems in BigDye® Terminator v3.1 Cycle Sequencing Kit (Part No. 4336921) protocol was followed in conjunction with a subsequent purification step utilizing a Biomek® NXP Laboratory Automation Workstation and the Agencourt® CleanSEQ kit protocol (Beckman Coulter, Brea, CA, USA).

Phylogenetic analyses. A phylogenetic analysis was undertaken to determine if the ITS1 through D1-D2 LSU

TABLE 1. Information on isolates used in this study. Original species designations, strain identification, origin, analyses performed (M, Morphology; T, Spirolide and PSP toxins; S, Sequence analyses), accession numbers and references to sequence and/or general information.

Orig. species design	Strain code	Origin	Source/Isolator	M	T	S	Genbank accession No.	Reference (sequences and/or general information)
A. ostenfeldii	AOF0901	Åland, Finland	A. Kremp	x	x	x	ITS: JX841282, LSU: X841308	This study
A. ostenfeldii	AOVA0917	Gotland, Sweden	A. Kremp	x	x	x	ITS: JX841276, LSU: JX841302	This study
A. ostenfeldii	AOKAL0909	Kalmar, Sweden	A. Kremp	x	x	x	ITS: JX841280, LSU: JX841306	This study
A. ostenfeldii	AOPL0917	Hel, Poland	A. Kremp	x	x	x	ITS: JX841277, LSU: JX841303	This study
A. ostenfeldii	K1354	Öresund, Denmark	SCCAP		x	x	ITS: JX841263, LSU: JX841289	This study
A. peruvianum	IEO-VGOAMD12	Palamos, Spain	I. Bravo	x	x	x	ITS: JX841266, LSU: JX841292	This study, Bravo et al. (2006)
A. peruvianum	IEO-VGOAM10C	Palamos, Spain	I. Bravo	x	x	x	ITS: JX841267, LSU: JX841293	This study, Bravo et al. (2006)
A. ostenfeldii	WW516	Fal River, UK	L. Percy	x	x	x	ITS: JX841256, LSU: JX841284	This study
A. ostenfeldii	WW517	Fal River, UK	L. Percy	x	x	x	ITS: JX841255, LSU: JX841283	This study
A. peruvianum	LSA06	Lough Swilly, Ireland	N.Touzet		x	x	ITS: JX841261, LSU: JX841288	This study
A. peruvianum	LSE05	Lough Swilly, Ireland	N.Touzet	x	x	x	ITS: JX841260, LSU: JX841287	This study
A. ostenfeldii	AONOR4	Oslofjord, Norway	A. Kremp	x	x	x	ITS: JX841279, LSU: JX841305	This study
A. ostenfeldii	NCH85	North Sea, Norway	T. Alpermann	x	x	x	ITS: JX841259, LSU: JX841286	This study
A. ostenfeldii	IMRV062007	North Sea, Norway					JF521637 (ITS and LSU)	Orr et al. (2011)
A. ostenfeldii	K0287	Limfjord, Denmark	SCCAP		x	x	ITS: JX841264, LSU: JX841290	This study, Hansen et al. (1992)
A. ostenfeldii	CCMP1773	Limfjord, Denmark	CCMP				JF521636 (ITS, LSU)	Orr et al. (2011)
A. ostenfeldii	CCAP1119/45	North Sea, Scotland	CCAP	x	x	x	ITS: JX841272, LSU: JX841298	This study
A. ostenfeldii	CCAP1119/47	North Sea, Scotland	CCAP	x	x	x	ITS: JX841271, LSU: JX841297	This study
A. ostenfeldii	S6_P12_E11	North Sea, Scotland	T. Alpermann		x	x	ITS: JX841257, LSU: JX841285	This study
A. ostenfeldii	S06/013/01	North Sea, Scotland	L. Brown		x	x	ITS: JX841258, LSU: GQ120505	This study, Brown et al. (2010)
A. ostenfeldii	BYK04	North Sea, Ireland	N.Touzet			x	ITS: JX841275, LSU: JX841301	This study
A. ostenfeldii	AOIS4	Breidafjord, Iceland	A. Kremp	x	x	x	ITS: JX841281, LSU: JX841307	This study
A. ostenfeldii	LKE6	G. of Maine, USA	D. Kulis	x	x	x	ITS: JX841262, LSU: EU707483	This study, Gribble et al. (2005)
A. ostenfeldii	HT120D6	G. of Maine, USA	D. Kulis		x	x	ITS: JX841268, LSU: JX841294	This study, Gribble et al. (2005)
A. ostenfeldii	HT120B7	G. of Maine, USA	D. Kulis	x	x	x	ITS: JX841269, LSU: JX841295	This study, Gribble et al. (2005)
A. ostenfeldii	F301	G. of Maine, USA	D. Kulis	x	x	x	ITS: JX841270, LSU: JX841296	This study, Gribble et al. (2005)
A. peruvianum	AP0704-2	New River, NC, USA	C. Tomas	x	x	x	ITS: JX878431, LSU: JX878433	This study
A. peruvianum	AP0704-3	New River, NC, USA	C. Tomas	x	x	x	ITS: JX878430, LSU: JX878432	This study
A. peruvianum	AP0411	New River, NC, USA	C. Tomas				JF921182 (ITS and LSU)	Tomas et al. (2012)
A. peruvianum	AP0905	Narraganset, USA	C. Tomas				JX113683 (ITS and LSU)	Borkman et al. (2012)
A. ostenfeldii	AOPC1	Saanich, Canada	A. Kremp	x	x	x	ITS: JX841278, LSU: JX841304	This study
A. peruvianum	IMPLBA033	Callao, Peru	S. Sanchez	x	x	x	ITS: JX841265, LSU: JX841291	This study
A. ostenfeldii	ASBH01	Bohai Sea, China	H. Gu	x	x	x	ITS: JN173268, LSU: JN173269	Gu (2011)
A. ostenfeldii	AOFUN0801	Hokkaido, Japan	S. Nagai				AB538439 (ITS and LSU)	Nagai et al. (2010)
A. ostenfeldii	AOFUN0901	Hokkaido, Japan	S. Nagai				AB538443 (ITS and LSU)	Nagai et al. (2010)
A. ostenfeldii	CAWD135	New Zealand	L. MacKenzie				ITS: AB753843, LSU: AB753841	Nagai et al. (2010)
A. ostenfeldii	CAWD136	New Zealand	L. MacKenzie				ITS: AB753844, LSU: AB753842	Nagai et al. (2010)

sequences fell into distinct groups corresponding to the morphologically defined species of the *A. ostenfeldii/A. peruvinaum* complex and to reveal the genetic relationships among the isolates. Prior to the phylogenetic analysis, the 37 ITS1 through D1-D2 LSU sequences (1,256 bp) obtained for each of the algal isolates were aligned using MAFFT (Multiple Alignment with Fast Fourier Transform; Katoh et al. 2009) as implemented in SeaView (Gouy et al. 2010). The default MAFFT settings were employed. Minor manual adjustments to the final alignment were performed using Chromas Pro (Version 1.5.). *A. minutum* and *A. insuetum* were used as outgroups. The resulting alignment is available upon request. An alternative RNA alignment was performed using the Multiple Alignment of RNAs tool (Smith et al. 2010) and representative ITS through D2 LSU sequences for *A. affine*, *A. andersoni*, *A. fundyense*, *A. insuetum*, *A. lusitanicum*, *A. minutum*, *A. peruvianum*, *A. ostenfeldii*, and *A. tamarense* from GenBank were used to guide the final alignment of the 37 combined ITS/D1-D2 LSU sequences.

Bayesian inference (BI) was performed using the software MrBayes v3.2 (Ronquist and Huelsenbeck 2003) with the GTR+G substitution model (Rodríguez et al. 1990), selected under the Bayesian Information Criterion (BIC) with jModelTest 0.1.1. (Posada 2008). For priors, we assumed no prior knowledge on the data. Two runs of four chains (three heated and one cold) were executed for 10,150 generations, sampling every 500 trees. In each run, the first 25% of samples were discarded as the burn-in phase. The stability of model parameters and the convergence of the two runs were confirmed using Tracer v1.5 (Rambaut and Drummond 2007). Additionally, a maximum likelihood (ML) phylogenetic tree based on the concatenated alignment was calculated in GARLI 2.0 (Zwickl 2006) with parameters estimated from the data, using an evolutionary model GTR+G, selected under the Akaike Information Criterion (AIC) with jModelTest 0.1.1. (Posada 2008). Tree topology was supported with bootstrap values calculated with 1,000 replicates.

In order to evaluate the full sequence diversity, we examined the extent of intra-strain variability in the LSU D1-D2 region (more D1-D2 sequences are available than are combined ITS/5.8S/D1-D2 sequences). The analysis included all currently available D1-D2 data from GenBank as well as those generated in this study. Though intra-strain rRNA variability was not obtained by our own analyses, as with other *Alexandrium* species (Orr et al. 2011), variant rDNA alleles were found within the genome of a single cell from sequences deposited to Genbank. The sequence data were first sorted and all unique sequences identified. These unique sequences were then aligned and analyzed phylogenetically as described above. The remaining sequences, which were identical to the unique sequences in the phylogeny, were subsequently added to the final phylogeny diagram (Table S1, in the Supporting Information).

To assess potential species level divergences (Litaker et al. 2007), genetic distances among the ITS sequences of the 37 *A. peruvianum and A. ostenfeldii* isolates (574 bp) were calculated with PAUP* 4.0a122 (Swofford 2003) using uncorrected genetic ("*p*"-distance) and GTR-model-based distances. A reticulate network was constructed by SplitsTree v 4.13 (Huson and Bryant 2006) using an agglomerative method, NeigborNet (NN; Bryant and Moulton 2004), with settings of character transformation using uncorrected *P*-values, equal angles and optimize box iterations set to 1.

Population structure and individual assignment were performed by a model-based clustering program, STRUCTURE v. 2 (Pritchard et al. 2000) using the ITS data set. Genotypes were sorted based on sequence similarity, with the parameters as follows: burn-in period of 10^6, MCMC repeat after burn-in, 30,000; admixture ancestry model.

ITS secondary structure analyses. Changes in the compensatory base pairing arrangements in the ITS2 region have been found to be a useful indicator of species level differentiation in green algae and a number of other protists groups (Coleman 2009). To determine if CBCs occur among the ITS2 sequences of *A. peruvianum* and *A. ostenfeldii* obtained in this study, we first estimated the secondary structure motif for these sequences using the RNA folding programs, RNAstructure ver. 5.0 (Mathews 2004) and Mfold (Zuker 2003) and universal ITS2 secondary structure motifs (Koetschan et al. 2010). The resulting motif was then used as template to construct other ITS2 structures by homology modeling (Model tool in ITS2 Database III, Koetschan et al. 2010). The ITS2 secondary structures were viewed and illustrated in VARNA ver. 3.7 (Darty et al. 2009).

Morphological observations and morphometric measurements. Twenty-nine isolates were examined morphologically. Specifically, cell size parameters, as well as the shapes and dimensions of the 1′, s.a. and 6″ plates (considered as diagnostic in the original species descriptions) were determined on 25 cells of four to eight isolates per phylogenetic group. Samples for morphological examination using light and epifluorescence microscopy were collected from exponentially growing cultures and preserved. A majority of the morphometric measurements and plate observations were performed on cells fixed with 1%–2% neutral Lugol's solution after confirming that preservation with this fixative had no significant effect on the plate appearance or measured values. To determine cell length and width, samples of fixed cells were placed under a Leica DMI3000B inverted microscope (Leica, Wetzlar, Germany) and photographed at 400× magnification with a Leica DFC 490 digital camera. Measurements were taken using the analysis tool of LAS (Leica Application Suite) camera software. Thecal plates were examined in epifluorescence after staining the Lugol fixed cells with a 1 mg $\cdot$ mL^{-1} solution of Fluorescent Brightener 28 (Sigma-Aldrich, St. Louis, MO, USA) according to the method of Fritz and Triemer (1985).

One way ANOVAs, followed by Tukey's HSD post hoc comparisons were performed using SPSS 15.0.1 software (IBM, Armonk, NY, USA) to test for differences in plate feature distributions and morphometric measurements between isolates and groups. When data were not normally distributed, the nonparametric Kruskal–Wallis test was applied.

Extraction and detection of PSTs. PSP toxin analyses followed the protocol described in detail by Hakanen et al. (2012). Cells from 30 mL of exponentially growing cultures were concentrated on Whatman GF/C filters (25 mm diameter). Filters were freeze-dried, and toxins were extracted in 1 mL of 0.03 M acetic acid, using an ultrasonic bath (Bandelin Sonorex Digitec, Berlin, Germany) at <10°C for 30 min. The filters were subsequently removed and the samples centrifuged at 12,000*g* for 5 min. The supernatants were then filtered through 0.45 μm GHP Acrodisc membrane filters (13 mm diameter; Pall Life Sciences, Port Washington, NY, USA). HPLC/FD analyses followed the protocol modified from Janiszewski and Boyer (1993) and Diener et al. (2006) as described in Hakanen et al. (2012). Analyses were performed using an Agilent HPLC system consisting of two series 1,100 pumps, degasser, autosampler, photodiode array, and fluorescence detector. The optical detectors were preceded by a high sensitivity dual electrode analytical cell 5011A (ESA, Chelmsford, MA, USA) controlled with an ESA Coulochem II multi-electrode detector to achieve electrochemical postcolumn oxidation (ECOS; Janiszewski and Boyer 1993). Fluorescence emission signal was used in the PST quantification.

The fluorescence detection was applied for the determination of PST oxidation products (Ex.: 335 nm, Em.: 396 nm, slits 1 nm). The samples were quantitatively analyzed by comparing with PSP standards purchased from the National Research Council Canada, Marine Analytical Chemistry Standards Program (NRC-CRMP), Halifax, Canada.

Spirolide analyses. For spirolide extractions, freeze-dried cell pellets from 30 mL of exponentially growing cultures were suspended in 500 μL deionized water and transferred to a spin-filter (pore-size 0.45 μm; Millipore Ultrafree, Eschborn, Germany) and centrifuged for 2 min at 800*g* (Eppendorf 5415 R, Hamburg, Germany) to remove salt. Filtrates were removed and 200 μL of methanol were added to the filters before incubation for 1 h. Filters were then centrifuged again for 2 min at 800*g*. The filtrates were transferred to HPLC vials and stored at −20°C until measurement.

Mass spectral experiments were performed on an ABI-SCIEX-4000 Q Trap (Applied Biosystems, Darmstadt, Germany), triple quadrupole mass spectrometer equipped with a TurboSpray® interface coupled to an Agilent (Waldbronn, Germany) model 1100 LC. The LC equipment included a solvent reservoir, in-line degasser (G1379A), binary pump (G1311A), refrigerated autosampler (G1329A/G1330B), and temperature-controlled column oven (G1316A). After injection of 5 μL of sample, separation of lipophilic toxins was performed by reverse-phase chromatography on a C8 column (50 × 2 mm) packed with 3 μm Hypersil BDS 120 Å (Phenomenex, Aschaffenburg, Germany) and maintained at 25°C. The flow rate was 0.2 mL · min^{-1} and gradient elution was performed with two eluents, where eluent A was water and eluent B was methanol/water (95:5 v/v), both containing 2.0 mM ammonium formate and 50 mM formic acid. Initial conditions were elution with 5% B, followed by a linear gradient to 100% B within 10 min and isocratic elution until 10 min with 100% B. The program was then returned to initial conditions within 1 min followed by 9 min column equilibration (total run time: 30 min).

Mass spectrometric parameters were as follows: curtain gas: 20 psi, CAD gas: medium, ion spray voltage: 5500 V, temperature: 650°C, nebulizer gas: 40 psi, auxiliary gas: 70 psi, interface heater: on, declustering potential: 121 V, entrance potential: 10 V, exit potential: 22 V, collision energy: 57 V. Selected reaction monitoring (SRM) experiments were carried out in positive ion mode by selecting the following transitions (precursor ion > fragment ion): m/z 534 > >150, 536 > >150, 540 > 164, 552 > 150, 628 > 150, 640 > 164, 644 > 164, 650 > 164, 658 > 164, 674 > 164, 678 > 150, 678 > 164, 692 > 150, 692 > 164, 694 > 150, 694 > 164, 698 > 164, 706 > 164, 708 > 164, 710 > 150, 720 > 164, 722 > 164, 766 > 164 and 784 > 164. Dwell times of 40 ms were used for each transition.

RESULTS

Phylogenetic analyses. BI and ML methods returned phylogenetic trees with identical topologies. In the BI tree shown in Figure 1, the *A. ostenfeldii*/*A. peruvianum* complex appears to be genetically highly structured with the sequences analyzed falling into six distinct phylogenetic groups. The clustering did not conform to the morphospecies distribution. Strains assigned morphologically to *A. peruvianum* and strains identified as *A. ostenfeldii* intermingled in the tree. Lower nodes were generally poorly resolved.

Analysis of larger D1-D2 LSU data sets focusing on unique sequences and intra-strain variability largely confirmed the initial analysis. In the D1-D2 phylogeny (Fig. 2), all the groups indicated in Figure 1 were present as separate highly supported (>0.95 branches except for the group 2 which had a branch support of only 0.73). Cloned rDNA sequences from the CCMP 1773 and APO411 isolates indicate that the amount of variation among alleles is small. The data also showed that the number of unique sequences was relatively small considering the number of isolates sequenced and that genetic differentiation among groups is small. In three of the clades (1, 2 and 6), an identical dominant allele was obtained from morphologically defined isolates of both *A. peruvianum* and *A. ostenfeldii*.

Group 1 contained a well-supported monophyletic group (ML 98%, BI 1.0) consisting of strains from different locations in the Baltic Sea (coasts of Denmark, Finland, Poland, and Sweden) and from estuaries at the U.S. East coast (New River, NC and Narragansett Bay, RI; Fig. 1). Although they were originally assigned to different morphospecies, Baltic (*A. ostenfeldii*) and U.S. (*A. peruvianum*) isolates had nearly identical sequences. The D1-D2 LSU phylogeny (Fig. 2) placed ASBH01 from Bohai Sea, China in the same subgroup, whereas the combined ITS/LSU phylogeny showed this strain to be divergent from all other group 1 strains.

Group 2, which was only supported by BI, but not ML (BI 0.9, ML 60%), consisted of isolates from coastal embayments and estuaries of Ireland, the Spanish Mediterranean, and the United Kingdom. Again, genetically closely related isolates had different morphospecific assignments (WW516 and WW517 as *A. ostenfeldii* and LSA06 and LSE05 as *A. peruvianum*).

Long branching isolates from Northern Japan formed a separate group, group 3 (BI 1.00, ML 100). Groups 4, 5, and 6 constituted a larger, well supported cluster that was distinct from the other groups. Group 4 contained strains from New Zealand (BI 1.00, ML 97%). Group 5 represents a monophyletic group of *A. ostenfeldii* strains originating from the NW Atlantic, mainly the Gulf of Maine (USA and Canada), but also from the NW coast of Iceland (Breidafjord) and the West coast of Norway. Group 6 (BI 1.00, ML 100%) consisted of a monophyletic group of *A. ostenfeldii* strains from the North Sea, isolated off the coasts of Denmark, Norway and Scotland. This group clustered together with two individually branching isolates from the Pacific coast of North America. One of these, IMPLBA033 with typical *A. peruvianum* morphology, was isolated from Callao, Peru, the type location of *A. peruvianum*. The other strain, AOPC1, originating from Saanich Inlet, Canada, was morphologically assigned to *A. ostenfeldii*.

Highest *P*-distances (Table 2; 0.067–0.083 substitutes) were detected between clade 6 and the Japanese isolates representing clade 3 (Table 2). While

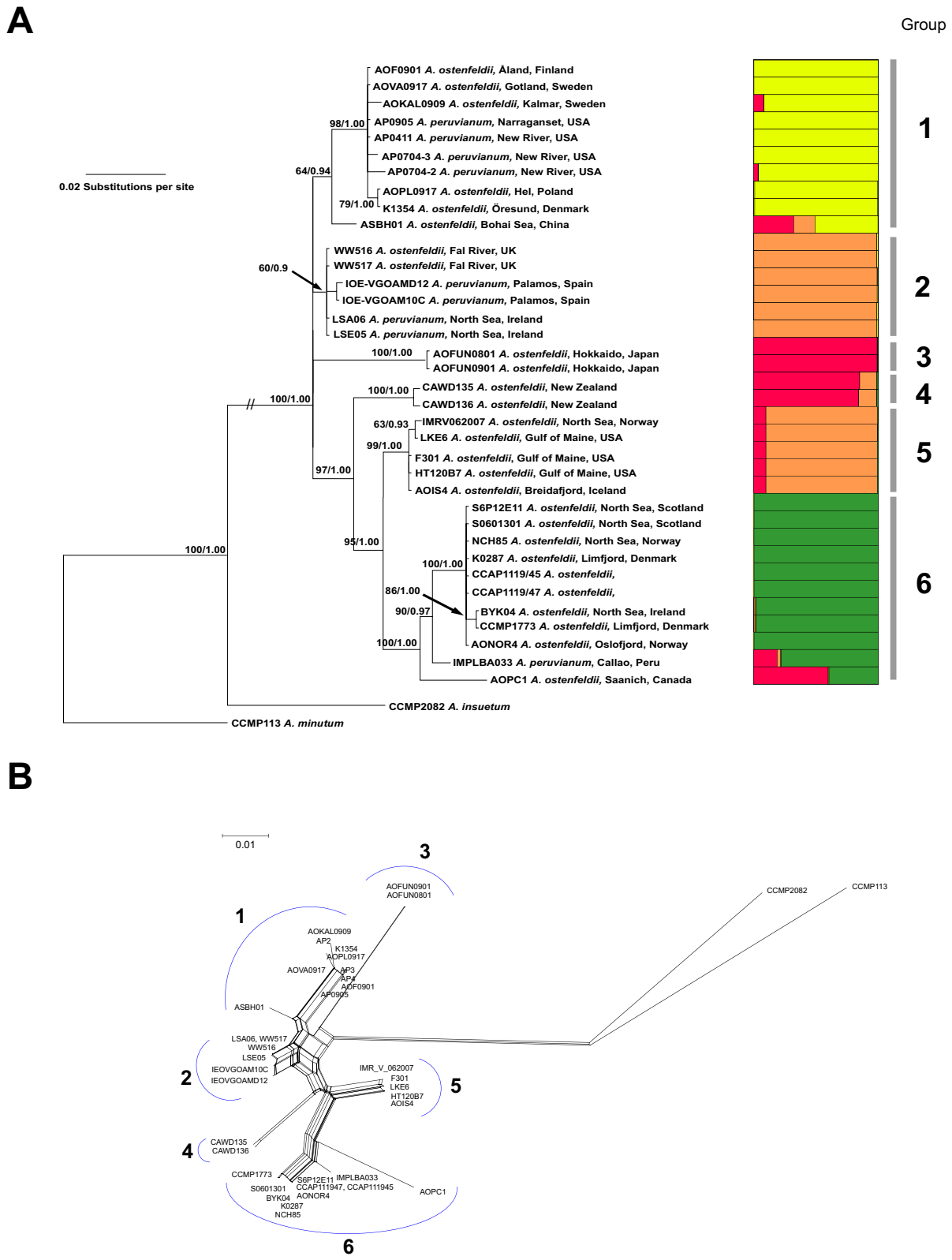

FIG. 1. Phylogeny of the *Alexandruim ostenfeldii* complex (A). Bayesian tree derived from a concatenated ITS1- 5.8S- ITS2 – D1/D2 LSU alignment (1,256 bp) including sequences of 37 strains. Node labels correspond to posterior probabilities from Bayesian inference, and bootstrap values from maximum likelihood, ML, analyses (ML/BI). Columns representing genotype clustering were generated with STRUCTURE hypothesizing K = 4. Species designations according to original morphospecies assignment (B) NeighborNet (NN) of *A. ostenfeldii* complex using SplitsTree, with edge lengths proportional to the uncorrected *P*-distances.

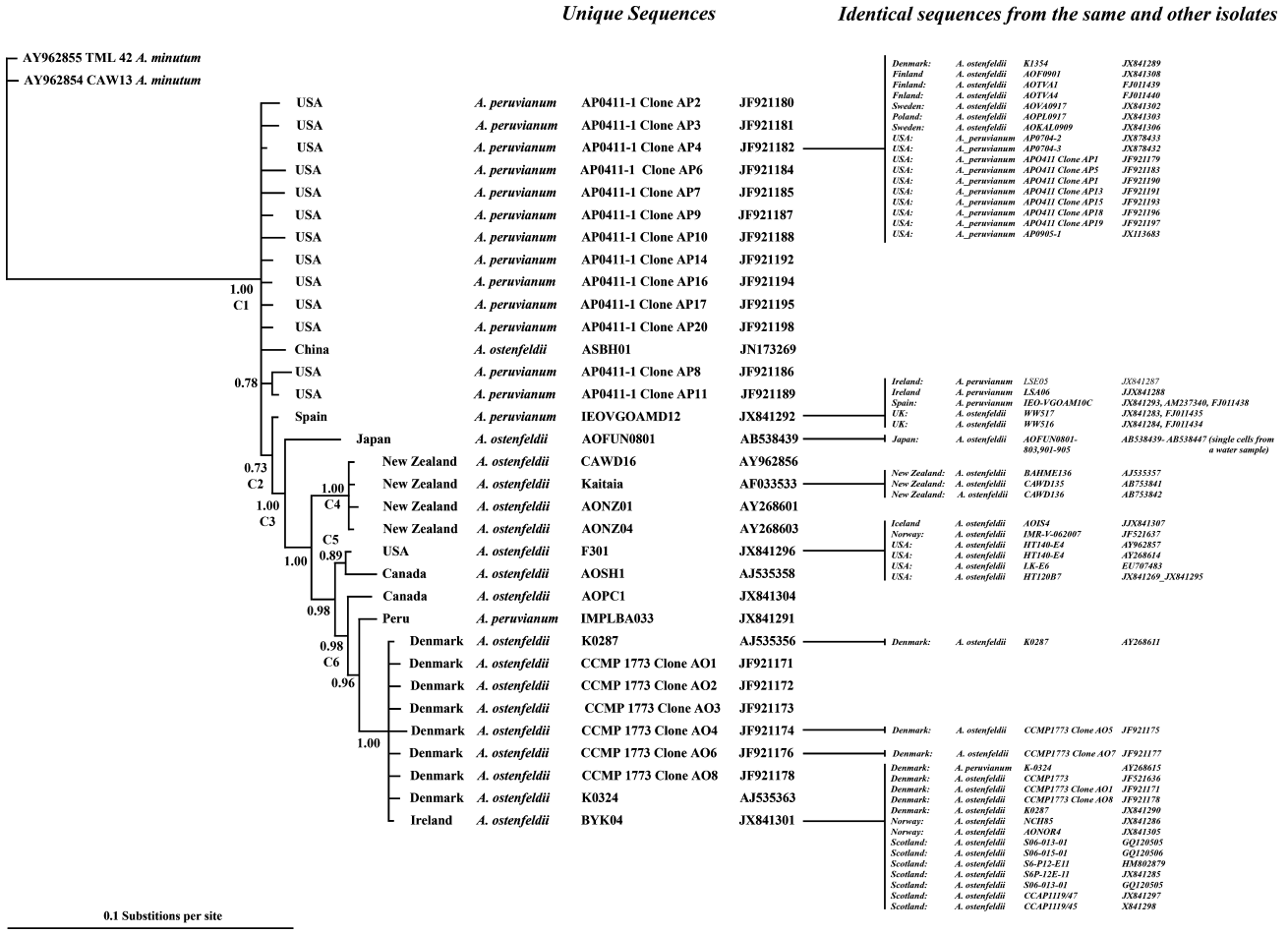

FIG. 2. Phylogeny constructed using the D1-D2 LSU sequences obtained from this study and from GenBank. *Alexandrium minutum* sequences served as an outgroup. The main phylogeny on the left was done using the 35 sequences, which were unique. Data provided for each sequence: the region of origin for the isolate from which the sequence was obtained, the morphological identification ascribed to that isolate, the isolate ID, and the GenBank accession number. The CCMP 1773 and APO411 clone designations represent PCR products from the same isolate, which were individually cloned and sequenced. The blocks of data on the right represent other sequences obtained in this study or GenBank which are identical – the sequence in the phylogeny is at the end of each horizontal line. The C1-C6 designations indicate the branches in this phylogeny, which correspond to the groups used in the original phylogeny (Fig. 1). Species designations according to original morphospecies assignments.

TABLE 2. Ranges of ITS distances (uncorrected *P*-distances, PAUP) within and among the six major genetic groups of *A. ostenfeldii*. *A. tamutum* was included as a comparative species closely related to the *A. ostenfeldii* complex.

	Group 1	Group 2	Group 3	Group 4	Group 5	Group 6
Group 1	0.000–0.019					
Group 2	0.015–0.030	0.000–0.005				
Group 3	0.046–0.058	0.042–0.048	0.000			
Group 4	0.040–0.056	0.030–0.033	0.062–0.063	0.032–0.033		
Group 5	0.036–0.053	0.025–0.030	0.065–0.067	0.000–0.002	0.004	
Group 6	0.050–0.076	0.035–0.056	0.067–0.083	0.039–0.055	0.028–0.046	0.000–0.033
A. tamutum	0.122–0.127	0.122–0.127	0.138	0.138–0.139	0.134–0.139	0.141–0.154

strains of clade 1 differed by 0.03–0.76 substitutions per site from all other clades, Clade 2 had an intermediate position, with approximately equal *P*-distances of 0.015–0.033 substitutions per site relative to clade 1, 4, 5, and most of clade 6 strains. Clades 4, 5, and 6 diverged from each other by 0.028–0.055 substitutions per site.

Concordance in the groupings was tested with the program, STRUCTURE. When *K* was set at 4, consistent groupings were noted (Fig. 1A). Extensive reticulation was observed within the grouping as inferred from the ITS NeighborNet (Fig. 1B). The network revealed six clusters corresponding to the groupings in the concatenated phylogeny (Fig. 1A).

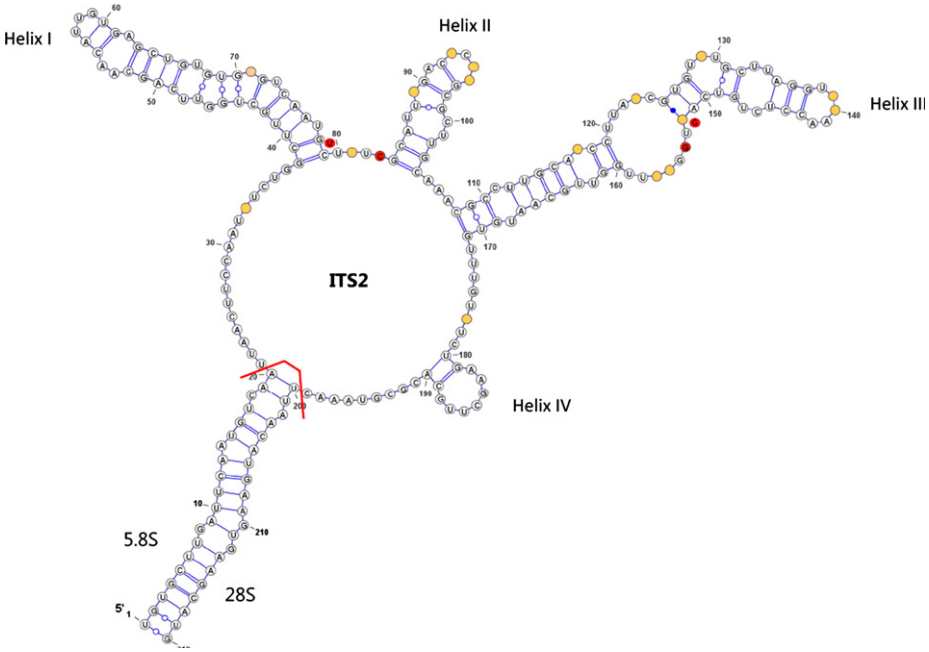

FIG. 3. Consensus secondary structure models of ITS2 in *Alexandruim ostenfeldii/peruvianum* based on 38 sequences showing high conservation. Nucleotides refer to the consensus character states. Circles in ochre show positions with base substitution, circles in red indicate indels. The proximal stem where 5.8S and 28S rRNA interacted is shown. Structural analysis of all 38 ITS2 sequences examined in this study showed the same folding pattern with no compensatory base changes.

Compensatory base changes in ITS2. The secondary structure of ITS2 revealed no CBCs among the 37 sequences of *A. ostenfeldii/A. peruvianum* that were analyzed. A consensus structure of ITS2 is shown in Figure 3. The transcripts revealed four universal helices (helix I–IV) in all ITS2 sequences analyzed, with conserved length, ranging from 168 to 171 nucleotides. The GC content in the helices ranged from 37% to 50%. The G–U pairings in helices were relatively low indicating high stability of helices (Fig. 3). A hemi-CBC was observed in AONOR4, NCH85, K0287, CCMP1773, CCAP1119/45 and 47, BYK04, S6_P12_E11, S06/013/01, AOPC1 and IMPLBA033; i.e., all the investigated strains belonging to group 6.

Cell size measurements. Cells size measurements of examined strains belonging to groups 1, 2, 5, and 6 are shown in Table S2, in the Supporting Information. Means of cell length, width, and the length/width (L/W) ratio varied considerably within and among strains of each group. All of the cultures examined contained both large and small cells as well as cells which were wider than long and vice versa. In group 1, the smallest strain, ASBH01, was approximately half the size of the largest strain, AOPL17, and the Baltic strains were on average more elongated with higher L/W ratios compared to the genetically nearly identical U.S. East coast strains. In group 2, cell size parameters varied significantly ($P < 0.05$) among the two Spanish strains (IEOVGOAM10C and IEOVGOAMD12) isolated from the same local population. The mean length and length/width rations of the group 5 strains were relatively uniform among strains (Table S2) size and shape but within strain variability was considerable. Group 6 contained the very small sized Norwegian strain AONOR4, but also a strain with large dimensions, AOPC1 from Pacific Canada. Though most strains of group 6 were slightly elongated, cells of the Peruvian strain IMPLBA033 were consistently wider than long. In general, within strain variation of size parameters was of the same magnitude as among strain variation.

Despite the large variability within and among strains, there were differences in the mean size of the different groups. The cells of groups 1 and 5, for instance, were significantly larger ($P < 0.05$) than cells of groups 2 and 6 when means of combined measurements of all cells and strains of each group were compared (Fig. 4A). Group means in the L/W ratio were comparable in groups 1, 2, and 6 (Fig. 4B) whereas the L/W ratio of group 5 cells was significantly higher ($P < 0.05$) than in cells of the other groups. Strains with a particularly low L/W ratio conformed mostly to the original *A. peruvianum* morphotype description. However, these characteristic dimensions were not consistently found within a given group or subset of groups.

Plate features. The first apical plate (1′) of nearly all of the analyzed cells had a straight upper segment of the right anterior margin (Fig. 5; Table 3), the only exception being strain IMPLBA033 from Peru (group 3), where the margin appeared curved (as typical for *A. peruvianum*) in the majority of cells. An extended upper segment of the 1′ plate as shown by Biecheler (1952) for *G. dimorpha* was common in five of the eight examined strains of group 1, however, a large fraction (between 33% and 55%) of cells of these strains also had a narrow 1′ plate (Fig. 5, A–C). In two strains within this group, AOKAL0909 and AOPL0917, the extension of the 1′ plate was observed only occasionally and in strain

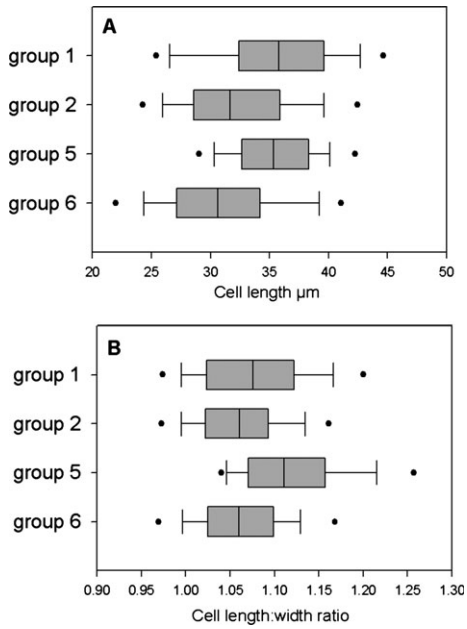

FIG. 4. Whisker diagrams for the replicate measurements of (A) cell length, and (B) the ratios of cell length to width, from all the strains representing groups 1–2 and 5–6. Isolates of groups 3 and 4 were not available for analysis. The line in the middle of each box represents the mean and the top and bottom of the box one SD from the mean Whiskers above and below the boxes indicate the 10th and 90th percentiles. The dots represent the 5th and 95th percentiles.

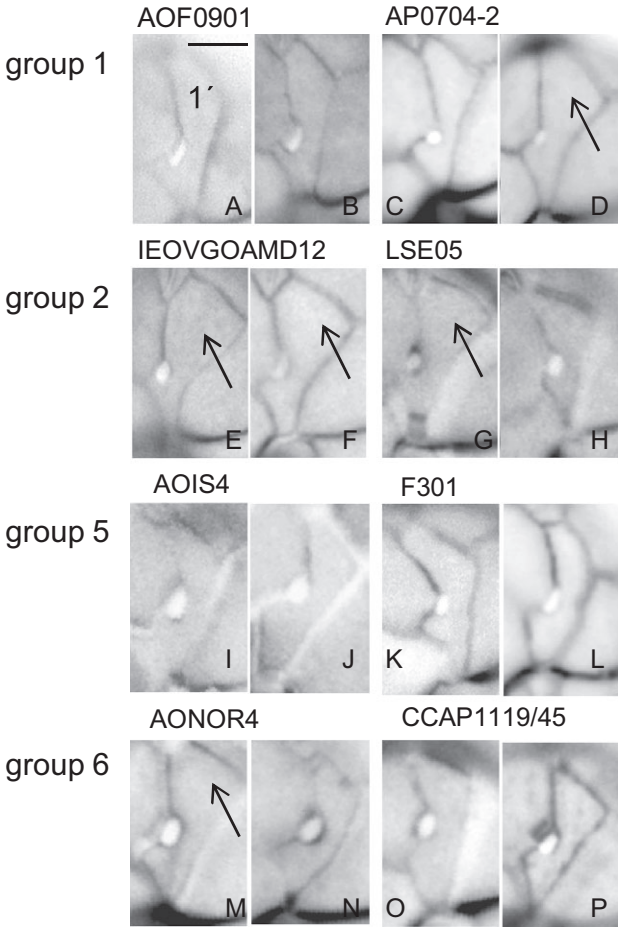

FIG. 5. Light micrographs of calcofluor stained 1′ plates from cells of two strains representative of the investigated groups showing variability in plate shapes. (A–D) Group 1 strains AOF0901 and AP0704-2; (E–H) group 2 strains IEOVGOAMD12 and LSE05; (I–L) group 3 strains AONOR4 and CCAP1119/45; (M–P) group 4 strains AOIS4 and F301. Scale bar (A) = 5 µm, arrows denote extensions.

ASBH01 it was completely absent. In group 2, a wide upper 1′ segment was consistently present (>80%) in all examined strains (Fig. 5, E–G). This feature was only occasionally found in strains of groups 5 and 6 (Fig. 5I). Here, the 1′ plate was usually narrow (Fig. 5, I–L and N–P). The frequency of extended upper 1′ segments was significantly higher in group 2 than in all other groups ($P < 0.05$). Group 1 differed significantly ($P < 0.05$) in frequency of the extension from groups 5 and 6, but also from group 2. Despite these statistical differences in frequency, the different 1′ morphologies, were exhibited by some strains in each group.

Differences were also noted among strains regarding the presence of a pointed versus flat posterior end of the 1′ plate where it contacts the s.a. plate (Fig. 5; Table 3). However, the distribution of this feature was not consistent within strains and groups. Generally, a pointed end was more commonly found in groups 5 and 6, where it was the dominant shape among cells of many, but not all strains. This was also the case in individual strains of groups 1 and 2 (ASBH01, IEOVGOAM10C). Despite being present in the majority of cells, there were always significant proportions of cells with a flat posterior 1′ end in each strain. The difference in the frequency of this feature was only significant between groups 1 and 6 ($P = 0.035$).

The area of the 1′ plate (Table 3) somewhat corresponded to the degree of upper segment extension. The 1′ area was significantly larger ($P < 0.05$) in group 2 compared to all other groups (Fig. 6A). Though the mean area was also larger in group 1, this difference was not significant due to the large variability of this feature in this group. Ventral pore (vp) size was variable within all groups as expressed by the large SD of group means (Fig. 6B; Table 3). However, group 1 mean was significantly lower ($P < 0.05$) compared to the other groups.

Evaluation of s.a. plate shapes revealed that both, door-latch (as typical for *A. ostenfeldii,* Fig. 7, A, F, G, I–K, and P) and A-shaped (as typical for *A. peruvianum,* including rounded shapes, Fig. 7, B–E, H, L–O) s.a. plates were present in most of the examined strains of all groups. In only 2 strains, AP0704-2 and IEOVGOAM10C did all s.a. plates belong to the A-shaped category. Generally, A-shaped s.a. plates were more common in groups 1 and 2 and door-latch-shaped s.a. plates in groups 5 and 6, though each shape was found in every group

TABLE 3. Distribution of distinctive plate features in representative strains of investigated phylogenetic groups.

Strain	Morpho type	1′ % straight	1′ % Ext.	1′ % pointed	1′ area (μm^2) Mean ± SD	vp area (μm^2) Mean ± SD	s.a.% A	s.a. % Door-latch	s.a. Ratio w/h Mean ± SD	6″ Ratio w/h Mean ± SD	*N*
Group 1											
AOF0901	*A. o.*	87	47	27	67.8 ± 11.8	2.67 ± 0.86	73	27	1.41 ± 0.24	1.15 ± 0.13	15
AOVA0917	*A. o.*	93	45	33	46.5 ± 10.5	1.77 ± 0.65	67	33	1.23 ± 0.19	1.12 ± 0.16	15
AOKAL0909	*A. o.*	100	25	7	43.2 ± 9.3	2.43 ± 0.66	20	80	1.39 ± 0.20	1.01 ± 0.09	15
AOPL0917	*A. o.*	93	13	13	76.7 ± 14.9	4.17 ± 0.82	73	27	1.40 ± 0.20	1.08 ± 0.08	15
AP0704-2	*A. p.*	73	53	40	64.9 ± 10.3	1.32 ± 0.31	100	0	1.19 ± 0.20	1.12 ± 0.10	15
AP0411	*A. p.*	93	65	20	71.6 ± 14.6	1.34 ± 0.80	75	25	1.10 ± 0.23	1.10 ± 0.14	15
AP0905	*A. p.*	93	67	42	59.1 ± 8.3	1.31 ± 0.45	80	27	1.13 ± 0.11	1.14 ± 0.13	15
ASBH01	*A. o.*	93	0	80	22.6 ± 3.0	0.87 ± 0.51	20	80	1.34 ± 0.26	1.45 ± 0.16	15
		91	**39**	**33**	**56.6 ± 18.0**	**1.99 ± 1.07**	**64**	**36**	**1.27 ± 0.23**	**1.10 ± 0.12**	
Group 2											
IEOVGOAM10C	*A. p.*	100	93	93	87.7 ± 18.8	4.20 ± 0.96	100	0	1.07 ± 0.21	1.20 ± 0.09	15
IEOVGOAMD12	*A. p.*	100	89	33	61.2 ± 15.5	2.26 ± 0.64	80	20	1.22 ± 0.16	1.17 ± 0.14	15
WW517	*A. o.*	100	87	12	56.1 ± 24.7	3.06 ± 1.11	69	31	1.31 ± 0.16	1.23 ± 0.18	15
WW516	*A. o.*	100	80	15	78.7 ± 16.7	3.31 ± 1.79	84	15	1.24 ± 0.29	1.12 ± 0.12	15
LS E05	*A. p.*	80	83	35	41.3 ± 6.7	1.76 ± 0.51	72	28	1.21 ± 0.15	1.17 ± 0.14	15
		96	**86**	**38**	**65.0 ± 18.4**	**2.92 ± 0.95**	**81**	**19**	**1.21 ± 0.20**	**1.19 ± 0.17**	
Group 5											
AOIS4	*A. o.*	100	20	60	55.6 ± 8.9	3.27 ± 0.60	45	55	1.31 ± 0.31	n.d.	8
F301	*A. o.*	93	0	36	47.4 ± 9.4	1.69 ± 0.56	8	92	1.53 ± 0.21	1.26 ± 0.13	15
LK6	*A. o.*	93	0	69	49.7 ± 16.0	3.06 ± 0.86	31	69	1.44 ± 0.38	1.38 ± 0.12	15
HT120B7	*A. o.*	100	17	50	49.2 ± 9.2	1.42 ± 0.66	40	60	1.60 ± 0.31	1.37 ± 0.07	5
		96	**9**	**54**	**50.5 ± 3.6**	**2.36 ± 0.94**	**31**	**69**	**1.46 ± 0.31**	**1.32 ± 0.13**	
Group 6											
AONOR4	*A. o.*	100	7	75	41.4 ± 5.3	2.77 ± 0.66	73	27	1.38 ± 0.17	1.38 ± 0.16	15
NCH85	*A. o.*	100	0	73	44.1 ± 8.8	2.90 ± 0.53	47	53	1.60 ± 0.19	1.33 ± 0.14	15
CCAP1119/45	*A. o.*	87	0	73	35.4 ± 5.9	2.12 ± 0.57	20	80	1.46 ± 0.16	1.34 ± 0.10	15
CCAP1119/47	*A. o.*	100	0	57	36.4 ± 7.0	2.19 ± 0.57	29	71	1.35 ± 0.16	1.35 ± 0.14	15
AOPC1	*A. o.*	100	0	47	66.3 ± 15.9	1.72 ± 1.18	20	80	1.41 ± 0.27	1.48 ± 0.20	14
IMPLBA033	*A. p.*	43	7	100	50.3 ± 8.5	2.05 ± 0.56	71	29	1.22 ± 0.12	1.26 ± 0.12	15
		88	**1**	**71**	**45.6 ± 11.5**	**2.29 ± 0.45**	**43**	**57**	**1.40 ± 0.21**	**1.35 ± 0.15**	

A. o. = *Alexandrium ostenfeldii* morphotype; A. p. = *Alexandrium peruvianum* morphotype, morphotypes as originally identified. Means for the clades are written in Bold.

(Table 3). For example, while most strains of group 1 had >70% A-shaped s.a. plates, 80% of the s.a. plates in strains AOKAL0909 and ASBH01were door-latch shaped. Similarly, group 6 isolates primarily exhibited door-latch s.a. plates whereas >70% of cells in strains AONOR4 and IMPLBA033 had A-shaped s.a. plates. Significant differences in the frequencies of diagnostic s.a. shapes were only detected between groups 2 and 5, with group 2 having significantly more ($P = 0.016$) A-shaped s.a. plates. Many of the A-shaped s.a. plates found in strains of group 1 were rounded (Fig. 7, B and C).

The width to height (W/H) ratios of the s.a. plate varied within and among strains (Fig. 8; Table 3). However, despite the large ranges within groups, the W/H ratios in groups 1 and 2 were on average significantly lower than those observed in groups 5 and 6 (Fig. 8; $P < 0.05$). Though significantly different, the group 6 s.a. W/H ratios appeared intermediate between groups 1 and 2 and group 5 (Fig. 8).

Width and height measurements of the 6″ plate revealed variable W/H ratios within and among strains (Table 3). Extremes were found in group 1, where strain AOKAL0909 consistently had large W/H ratios and strain ASBH01 – exhibited uniformly low W/H ratios. Overall, the 6″ plate W/H ratios were generally lower in groups 1 and 2 compared to groups 5 and 6 (Fig. 9; $P < 0.001$).

Toxin composition. Of all strains analyzed for PSP toxins and spirolides, only AOPC1 from Saanich Inlet, Canada, did not contain measurable amounts of PSTs or spirolides. While all strains of group 1 contained PSP toxins, IMPLBA033 was the only PST producer of groups 2, 5, and 6 (Table 4). The Baltic strains produced only GTX2/3 and STX, whereas additional analogs C1/C2 and B1 were detected in the estuarine strains from the U.S. East coast. The Chinese Isolate contained NEO in addition to STX. High amounts of GTX2/3 and STX were found in the Peruvian isolate.

Spirolides were measured in isolates from all analyzed groups (Fig. 10). In group 1, only the U.S. East coast strains contained spirolides. These, as well as all group 2 isolates produced predominantly (>99%) 13dmC spirolide. The group 2 isolates also produced low amounts of 13,19ddmC (UK isolates) and spirolide A (UK and Spanish strains). Group 5 strains produced a mixture of different spirolides, primarily spirolides A (Gulf of Maine strains) and C (AOIS4 from Iceland). In group 6, the North Sea strains contained considerable amounts of spirolides,

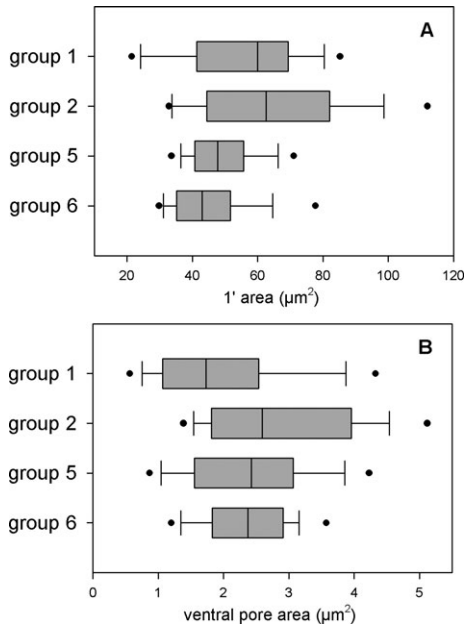

FIG. 6. First apical (1′) plate features from all the strains representing groups 1–2 and 5–6. Isolates of groups 3 and 4 were not available for analysis. The line in the middle of each box represents the mean and the top and bottom of the box one SD from the mean Whiskers above and below the boxes indicate the 10th and 90th percentiles. The dots represent the 5th and 95th percentiles.

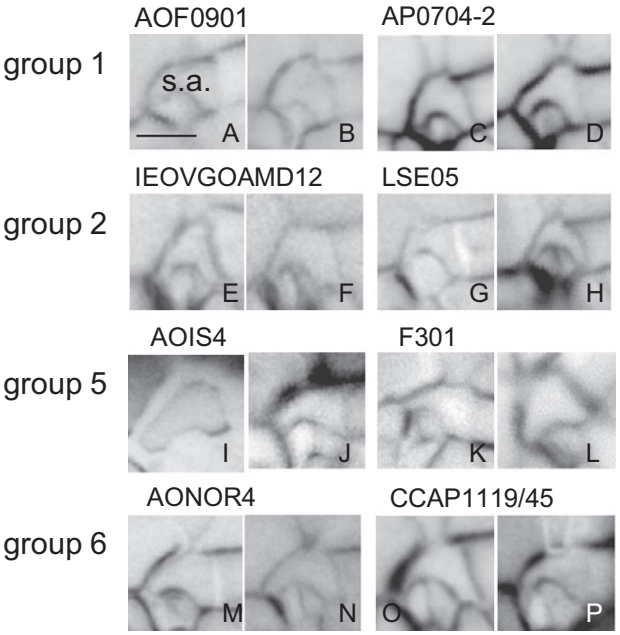

FIG. 7. Variability in s.a. plate shapes. Light micrographs of calcofluor stained s.a. plates from different cells of two strains representative of four groups investigated in this study. (A–D) group 1 strains AOF0901 and AP0704-2; (E–H) group 2 strains IEOVGOAMD12 and LSE05; (I–L) group 3 strains AONOR4 and CCAP1119/45; (M–P) group 4 strains AOIS4 and F301. Scale bar (A) = 5 μm.

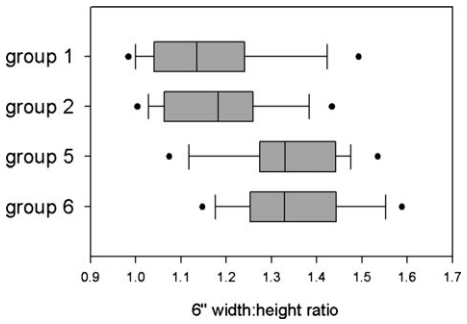

FIG. 8. Whisker diagram of s.a. plate width to height ratios from all the strains representing groups 1–2 and 5–6. Isolates of groups 3 and 4 were not available for analysis. The line in the middle of each box represents the mean and the top and bottom of the box one SD from the mean Whiskers above and below the boxes indicate the 10th and 90th percentiles. The dots represent the 5th and 95th percentiles.

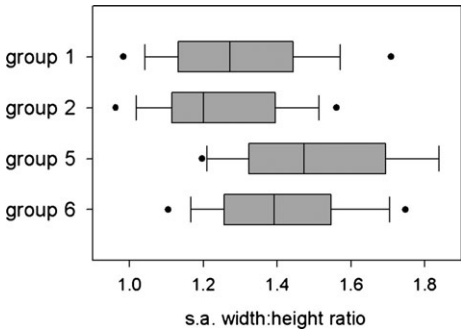

FIG. 9. Whisker diagram width to length ratios of the 6th precingular (6″) plate from all the strains representing groups 1–2 and 5–6. Isolates of groups 3 and 4 were not available for analysis. The line in the middle of each box represents the mean and the top and bottom of the box one SD from the mean Whiskers above and below the boxes indicate the 10th and 90th percentiles. The dots represent the 5th and 95th percentiles.

mainly 20mG and G. The main exception was AONOR4 which produced mostly 13,19ddmC and CCAP1119/47 which had significant amounts of spirolide A in addition to G. All group 6 strains contained small proportions of other spirolide forms.

DISCUSSION

Molecular phylogeny and morphospecies concept. This study represents the first comprehensive investigation of phylogenetic, morphological, and toxin relationships in a broad set of isolates assigned to *A. ostenfeldii* and *A. peruvianum*. Phylogenetic analysis of rDNA sequences from the *A. ostenfeldii* or *A. peruvianum* cultures examined in this study revealed a complex genetic structure, consisting of six distinct, but closely related groups. A detailed qualitative and quantitative analyses of isolates belonging to four of these groups showed that the

TABLE 4. Distribution of Saxitoxin analogs in strains containing PSP toxins.

Strain	Group	C1/2	GTX2/3	B1	STX	NEO	Reference
AOF0901	1	–	+	–	+	–	This study
AOVA0917	1	–	+	–	+	–	This study
AOKAL0909	1	–	+	–	+	–	This study
AOPL0917	1	–	+	–	+	–	This study
K-1354	1	–	+	–	+	–	This study
AP0704-2	1	+	+	+	+	–	This study
AP0704-3	1	+	+	+	+	–	This study
AP0411	1	+	+	+	+	–	Tomas et al. (2012)
AP0905	1	+	+	+	+	–	Borkman et al. (2012)
ASBH01	1	–	–	–	+	+	This study
IMPLBA033	3	–	+	–	+	–	This study

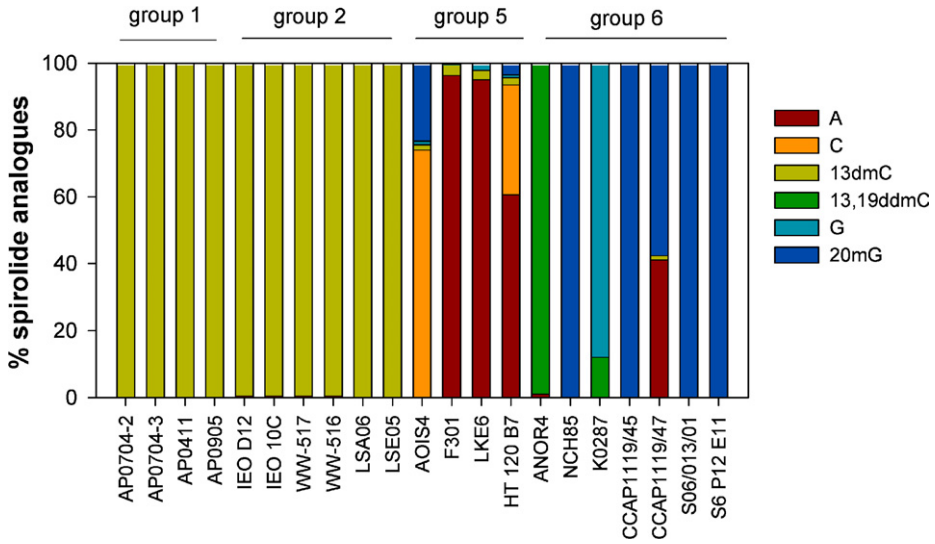

FIG. 10. Percent distribution of spirolide analogs in strains with measured spirolide production.

diagnostic morphological characters (shape differences in the 1′, s.a. and 6″ plates) used to define the original species were more variable than previously assumed, exhibiting extensive intra- and inter-strain variability. Instead of the morphological features being consistently associated with a given group, as would be expected if *A. ostenfeldii* and *A. peruvianum* were distinct species, each group examined contained strains morphologically identified as either *A. ostenfeldii* or *A. peruvianum*.

In group 1, for instance, Baltic *A. ostenfeldii* and North American *A. peruvianum* strains (as identified by Kremp et al. 2009, Borkman et al. 2012, Tomas et al. 2012) form a monophyletic subgroup in the phylogenetic tree (Fig. 1). Two nearly identical sequences were obtained from *A. ostenfeldii* (AOKAL0909) and *A. peruvianum* (e.g., AP0905). Also, strains from the type localities of *A. ostenfeldii* and *A. peruvianum* were closely nested in the same phylogenetic group, group 6. Strain IMPLBA033, which represents the type location of the species in Callao, Peru (Balech and de Mendiola 1977) and which is morphologically in accordance with the *A. peruvianum* description, appears as the immediate neighbor of AONOR4, an *A. ostenfeldii* strain isolated from the location of the *A. ostenfeldii* redescription in Norway (Balech and Tangen 1985). The strain AOIS4 from the Iceland where Paulsen first found the species, was nested in group 5. AONOR4 in contrast, more closely resembles the description of *A. peruvianum* than the type described from the same location. Thus, though the *A. ostenfeldii* and *A. peruvianum* morphotypes as originally described appear distinct, their often nearly identical rDNA sequences indicate they represent the extreme ends in a continuum of *A. ostenfeldii* morphotypes. Consistent with this conclusion, the isolates examined in this study often showed a combination of the type *A. ostenfeldii* and *A. peruvianum* morphologies.

Morphological characters were generally not consistently distributed. AONOR4 has some features that are typical for *A. peruvianum* such as small cell size and a predominantly A-shaped s.a. plate, which is not in accordance with what Balech and Tangen (1985) observed in field samples, collected from the same location. Cells of the Peruvian strain, on the other hand, were not particularly small as originally reported in the species description. The most inconsistent character, considered diagnostic in the original description, is the curved right anterior margin

of the 1′ plate of *A. peruvianum*. Such curved margin was only found in one of the investigated seven strains assigned to *A. peruvianum*, IMPLBA033 from Peru, and in none of the *A. ostenfeldii* strains. The suitability of this character for identification of *A. peruvianum* has been previously challenged, e.g., by Lim et al. (2005), who found a large number of cells with a straight margin in material from Malaysia that otherwise agreed with the *A. peruvianum* description. Balech (1995) similarly reported a mix of straight and curved margins in material from North America; however, he considered this an exception. The s.a. plate, which has commonly been considered the most important feature for the delineation of *A. peruvianum* from *A. ostenfeldii* (Balech 1995, Lim et al. 2005, Bravo et al. 2006, Touzet et al. 2011, Tomas et al. 2012), was also found to be problematic. Most of the *A. peruvianum* isolates contained significant amounts (20%–30%) of the door-latch shaped s.a. plates typical for *A. ostenfeldii*. A-shaped "*A. peruvianum*"- s.a. plates, in turn, were present in most *A. ostenfeldii* strains, often >40% of the cells from the same culture frequently exhibited this feature. Such reverse s.a. distributions were furthermore observed in closely related strains from the same geographic population. In the Baltic Sea, for example, the geographically and genetically close strains AOKAL09 and AOVA17 had 20% and 67% A-shaped s.a. plates, respectively. Such intra-strain and within population/group variability also calls into question the applicability of the s.a. shape as a distinctive character.

Finally, distinctive *A. peruvianum* features rarely occurred in combination, i.e., A-shaped s.a. plates were not necessarily accompanied by small ventral pores or smaller cell size. Our observations on extensive material from a large global sample set emphasize that the present morphological delineation of *A. peruvianum* from *A. ostenfeldii* is not well supported. Together, phylogenetic and morphological data suggest that *A. peruvianum* should not be considered a distinct species, and that the name should be treated as synonym of *A. ostenfeldii*.

Genetic differentiation. Each of the analyses returned six phylogenetic groups. These results were consistent with previous phylogenetic analyses based on either concatenated rDNA (Orr et al. 2011) or LSU D1-D2 (Anderson et al. 2012) sequences. Typically, the groups fell into two main clusters, with those corresponding to groups 4, 5 and 6 forming one and groups 1 and 2 another. Prior to the more detailed analysis in this study, it had been suggested that the *A. ostenfeldii* complex contained two major genetic groups or genotypes (Touzet et al. 2008, Kremp et al. 2009) that may even coexist (Touzet et al. 2008). The results of this study indicate that instead of two clearly differentiated genotypes, the groups represent a continuum of ribotypes which are differentiated both morphologically and genetically from one another by varying degrees. Consistent with this view, depending on which RNA region is analyzed and the phylogenetic analysis method employed, the actual order in which various groups appear varies. LSU alignments typically cluster groups 1 and 2 together, whereas ITS alignments sometimes return trees where group 2 strains cluster together with groups 4, 5, and 6 (Gu 2011, Tahvanainen et al. 2012). In the concatenated phylogeny presented here, group 1 appears clearly differentiated, whereas the branching of group 2 is poorly resolved, which emphasizes its low divergence from the respective other groups and puts it into an intermediate position between group 1 and groups 4/5/6.

Although the present strain sampling is not fully representative of the global distribution of the *A. ostenfeldii* complex, the rDNA analysis indicates some ecological and phylogeographic patterns. Groups 1 and 2 both contain a mix of geographic isolates from shallow and productive coastal embayments or river estuaries (Percy et al. 2004, Bravo et al. 2006, Kremp et al. 2009, Tomas et al. 2012, Table 1). Laboratory studies have shown that many group 1 isolates show optimal growth under mesohaline conditions (Gu 2011, Suikkanen et al. 2013). In contrast, group 2 strains were isolated from higher salinity environments and have been shown to exhibit optimal growth at near oceanic salinities (Suikkanen et al. 2013).

Baltic *A. ostenfeldii* strains have recently been considered a distinct lineage that has evolved due to physical and physiological barriers after the last glaciation in the newly formed enclosed brackish water body of the Baltic Sea (Tahvanainen et al. 2012). However, this scenario must be reconsidered given that identical genotypes have been isolated from the U.S. East coast. The close genetic relationships of these geographically distant populations suggest recent anthropogenic dispersal as documented for a number of toxic phytoplankton species (e.g., Bolch and de Salas 2007). Population genetic analyses of Baltic *A. ostenfeldii* using AFLP showed significant isolation by distance within the Baltic Sea, implying that the species has been present here for a long period of time (Tahvanainen et al. 2012).

The ecophysiological data available for isolates belonging to groups 3–6 are less comprehensive, but the established salinity tolerance ranges are narrow and clearly indicate adaptation to marine conditions (Suikkanen et al. 2013). In these groups, genetic relationships more clearly reflect geographic distribution patterns. Group 3 and 4 may represent geographically isolated populations with group 3 from Japan possibly being a distinct East Asian genotype and group 4 containing isolates from New Zealand. Closely related groups 5 and 6 consist to a large part of strains from the North Atlantic with group 5 strains representing the western parts and group 6 strains the eastern coasts. However, it is likely that with additional sampling the observed

pattern may change and some groups will be found to be globally distributed. This conclusion is supported by the distribution of group 6 isolates, which occur in both the North Atlantic and the west coast of Canada and Peru.

Trait distribution among phylogenetic groups. Despite the considerable intra- and inter-strain variability in morphological characters, morphometric measurements and frequencies of some plate features were significantly related to phylogenetic structure. Frequencies of s.a. plate shapes as well as width/height ratios of the s.a. and 6″ plates differed statistically between groups, specifically groups 1/2 and groups 5/6. Though these plate features were not consistently present or absent, their quantitative distribution in these groups, indicates some degree of isolation. Particularly conspicuous was the frequent occurrence of an anteriorly extended 1′ plate in groups 1 and 2 (also reflected by a larger 1′ area in these groups), a feature described by Biecheler (1952) for *G. dimorpha*. This feature has previously gone unnoticed due to the fact that most researchers have not considered the possibility that *G. dimorpha* may actually represent an *Alexandrium* species, despite the undeniable similarity to *A. ostenfeldii and A. peruvianum*. Balech's doubts concerning the identity of *G. dimorpha* (Balech and Tangen 1985, Balech 1995), motivated by the large variety of cell and plate shapes in Biecheler's illustrations (Biecheler 1952), have possibly contributed to the lack of recognition. Another factor that may be involved is sampling bias. Small coastal lagoons like the one Biecheler investigated have only very recently come to the attention of scientists as potential *A. ostenfeldii/peruvianum* habitats due to toxic *A. ostenfeldii* or *A. peruvianum* blooms (Kremp et al. 2009, Borkman et al. 2012). The cells described recently from "*G. dimorpha*" habitats frequently show typical group 1 and 2 features, most conspicuously the anteriorly extended 1′ plate (Bravo et al. 2006, Kremp et al. 2009, Borkman et al. 2012, Tomas et al. 2012, figs. 1, 10 and 11). It is likely that our groups 1 and 2 represent what Biecheler described as *G. dimorpha*. This idea is further strengthened by the fact that the two Spanish group 2 strains IEOVGOAMD12 and IEOVGOAM10C were isolated from an embayment at the Catalan coast, only 200 km south of the *G. dimorpha* type location.

The morphologies of group 5 and 6 strains, which comprise much of the other larger phylogenetic cluster, conformed mostly to the *A. ostenfeldii* description. Morphometric data revealed high frequencies of typical features such as narrow 1′ plates, door-latch-shaped s.a. plates and wide 6″ plates. These strains predominantly originate from the regions in the vicinity of the type location in Iceland (Paulsen 1904) and Norway. Specifically, AOIS4 isolated for this study from Breidafjord, Iceland, fits the type as defined by Balech and Tangen (1985) quite well with mostly narrow 1′ plates, frequently occurring low door-latch-shaped s.a. plates and a large ventral pore. The third group of the cluster, group 4, consists of isolates from New Zealand that were not further investigated here. Material from this area has, however, been documented extensively (MacKenzie et al. 1996, 2004) and the respective analyses indicate high morphological similarity with groups 5 and 6 isolates and the *A. ostenfeldii* morphotype.

Genetic distinctions among the different groups and larger clusters were further reflected by differences in toxin composition, particularly spirolide profiles. PSP toxins were mainly and most consistently encountered in group 1 of which all strains produced saxitoxin analogs. The composition of STX analogs was not related to specific genotypes, but varied according to geographic distribution, as Baltic strains consistently produced a different suite of PSTs as compared to genetically similar East U.S. coast strains and the Chinese isolate. PSP toxins were less common in the other groups, where only one of the examined strains, IMPLBA033 from Peru, contained PSTs. Hence, presence of PSTs might be considered as a characteristic trait of group 1. However, the present analysis cannot be regarded as fully representative of the PST distribution within the *A. ostenfeldii* complex. PST production is, for example, common in group 4 constituting *A. ostenfeldii* from New Zealand (MacKenzie et al. 1996), a group closely related to groups 5 and 6. Furthermore, low cellular concentrations of PSTs have been reported previously from several group 6 strains – Danish K-0287 (Hansen et al. 1992) and Scottish S06/013/01 (Brown et al. 2010) – found negative in our analysis. It has been discussed that the ability to produce PSTs may be lost in culture (Martins et al. 2004, Orr et al. 2011). Suikkanen et al. (2013) reported the presence of one of the two *sxtA* gene motives (*sxtA*1) involved in saxitoxin production (Stüken et al. 2011) from non-PST producing strains NCH 85 and S6/013/01, indicating that a genetic basis for PST production in group 6 strains exists, but is not operational (Stüken et al. 2011, Hackett et al. 2013).

In contrast to PST distribution, spirolides were detected in strains from all investigated phylogenetic groups, and their composition was clearly in accordance with the group structure. All spirolide producing strains of groups 1 and 2 contained almost exclusively 13dmC whereas groups 5 and 6 strains had diverse toxin profiles and other dominant spirolide analogs. Interestingly, spirolide composition differed quite considerably between groups 5 and 6 despite their close genetic relationship and the geographic proximity of their representative isolates. Spirolide profiles have been considered to be relatively conserved when measured at comparable growth state and thought to be insensitive to environmental change (MacLean et al. 2003, Suikkanen et al. 2013). The analyses presented here confirm the results of earlier spirolide profile characterizations

and put them into a phylogenetic context. For example, 13dmC was found in locations and in strains representative of groups 1 (Van Wagoner et al. 2011) and 2 (Percy et al. 2004, Ciminiello et al. 2006, Franco et al. 2006, Touzet et al. 2008), while 20mG or G dominance in North Sea group 6 strains is reflected in reports from that area (Aasen et al. 2005, Krock et al. 2007, Brown et al. 2010). Reports from the western North Atlantic show a prevalence of spirolide A (Gribble et al. 2005). This emphasizes the potential relevance of spirolide profiles as chemical markers.

Representatives of the *A. ostenfeldii* complex are the only known *Alexandrium* species that produce several toxins at the same time: Isolates from the U.S. east coast river estuaries produce PSTs', spirolides and 12 methylgymnodimine (Van Wagoner et al. 2011, Tomas et al. 2012). However, as shown here, a number of strains only produce spirolides while others contain only PSTs. Investigations on the effects of salinity showed that at least PST production is genetically predetermined (Suikkanen et al. 2013). Interestingly, unidentified cyclic imines related to gymnodimines and/or spirolides, have been detected in low abundances in Baltic isolates (Bernd Krock, unpublished) suggesting that spirolide synthesis pathways are to some extent established also in nonspirolide producing strains.

Species boundaries. The apparent relationships of genetic structure and phenotypic trait distribution raise the question whether groups or larger phylogenetic entities should be considered distinct species. As elucidated above, many of the group 1 and 2 strains resemble *G. dimorpha* morphologically while the cluster containing groups 4/5/6 is characterized by predominance of *A. ostenfeldii* plate features. Nevertheless, consistent morphological distinction of groups 1 and 2 from the *A. ostenfeldii* morphotype cluster is not evident. The main differentiating feature, the anteriorly extended 1′ plate that was found in >80% of cells of group 2 (compared to on average <10% of groups 5 and 6 cells), was much less frequently observed in group 1 strains. Instead, the latter strains mostly contained a mix of wide and narrow plates. Group 1 thus takes an unresolved morphological position between the *A. ostenfeldii* and *G. dimorpha* morphotypes represented by groups 4/5/6 and group 2, respectively.

If morphological distinction of group 2 from 4/5/6 coincided with strong genetic differentiation, segregation of these entities as distinct species, *G. dimorpha* and *A. ostenfeldii* could still be considered together with the possibility that group 1 represents a hybrid. Molecular analyses identified group 2 as a genetic intermediate with an unresolved genetic affiliation. The genetically transitional state of group 2 suggested by the short or unstable branching in phylogenetic analyses is emphasized by the low uncorrected *P*-distances of group 2 sequences from the genetically more divergent groups 1 and 3–6. Since genetic differentiation is apparently not compatible with the morphospecies concept of *G. dimorpha,* the indicated morphological species boundaries cannot be substantiated. This again implies that *G. dimorpha* should not be considered a distinct species within the *A. ostenfeldii* complex but a synonym of *A. ostenfeldii*.

The data in this study indicate the *A. ostenfeldii* complex either represents one phenotypically variable phylogeographically structured species or else a series of cryptic species, i.e., genetic species that are morphologically not defined. The latter scenario has been suggested for the *A. tamarense* group which shows strong intraspecific genetic differentiation. This differentiation is, however, not coupled to phenotypic or morphological traits (Lilly et al. 2007, Orr et al. 2011). In the *A. ostenfeldii* complex, ITS divergence data might be interpreted in favor of the latter hypothesis. That is, mean ITS uncorrected *P*-distances of >0.04 were detected between group 1 and groups 3–6, which reflects species level differentiation seen in some dinoflagellates (Litaker et al. 2007). Groups 1 and 2, as well as groups 3, 4, and 5 on average also fell below the 0.04 substitutions per site level. The genetic variation among the remaining group comparisons was higher, with group 6 consistently being the most divergent. However, in every case except for one pair of sequences from clades 3 and 6, the uncorrected genetic distances fall below the most conservative divergence threshold of 0.08 substitutions, indicating species level divergence in species with rapidly evolving sequences. Hence, ITS data are consistent with either a higher than average divergence rate in the ITS region of *A. ostenfeldii* or the possible existence of several cryptic species which are morphologically indistinguishable.

To better understand if groups represent cryptic species, we considered whether there was any evidence among the isolates for reproductive incompatibility consistent with the biological species concept. In many dinoflagellates reproductive isolation can be determined using mating studies that assess the ability to produce viable offspring. Unfortunately, in contrast to other *Alexandrium* species, *A. ostenfeldii* often produces resting cysts by homothallic and/or asexual reproduction (Østergaard-Jensen and Moestrup 1997, Figueroa et al. 2008). Hence, cyst formation cannot be considered as an unambiguous indicator of sexual compatibility. In this study, potential reproductive isolation was assessed by comparing the secondary structure of ITS2 transcripts. This approach was taken because nucleotide identity in helix III of ITS2 is considered an indication of sexual compatibility (Coleman 2009) whereas the presence of CBCs suggests sexual incompatibility. Hence, CBCs may guide the evaluation of species boundaries, particularly when genetic and/or morphological data are ambiguous. In microalgae, CBC analyses have been used to establish

cryptic species, e.g., in the diatom genus *Pseudo-nitzschia* (Amato et al. 2007, Quijano-Scheggia et al. 2009) and dinoflagellates in the genus *Coolia* (Leaw et al. 2010). The CBC analyses revealed absence of any CBCs in the entire sequence set (43 sequences) examined in this study. This suggests that all groups are able to interbreed. Hemi-CBCs were consistently found in strains of group 6, which might be interpreted as a sign of beginning reproductive isolation (Coleman 2009). Terminal group 6 might thus represent a genetically differentiated population that could eventually give rise to a new species.

Conclusions. The finding of inconsistent morphological and gradual genetic divergence of groups together with no evidence of CBCs indicating reproductive isolation, supports the interpretation that the *A. ostenfeldii* complex represents one species: *A. ostenfeldii*. Based on the inconsistencies of the *A. peruvianum* and *G. dimorpha* morphotype distributions we propose that *A. peruvianum* and *G. dimorpha* should be discontinued as species names and treated as synonyms of *A. ostenfeldii*. These conclusions are in agreement with the present criteria used for species delimitation in dinoflagellates and recent considerations on species boundaries in the genus *Alexandrium*. Mostly for practical reasons, present dinoflagellate taxonomy, and protist diversity in general (Boenigk et al. 2012), still considers consistency of morphological characters an important aspect in species definition. Hence, the above discussed inconsistencies in distinctive morphological characters are a strong motivation for a decision in favor of a broad species concept of *A. ostenfeldii*. Molecular data considered in relation to other *Alexandrium* species supports this concept: Allelic variation found among isolates is small, clearly reflecting divergences within rather than among presently defined *Alexandrium* and other dinoflagellate species (Litaker et al. 2007 and Litaker et al. 2009, Orr et al. 2011). Also, the lack of full CBCs in the ITS2 transcripts in the *A. ostenfeldii* groups supports a broad species definition when considered in relation to other dinoflagellates, where presence of CBCs support separation of morphologically and genetically differentiated entities at species level (Leaw et al. 2010).

Although our conclusion is based on a number of different criteria and the best presently available sample material, it cannot be excluded that, with more data and more and refined criteria for species delimitation at hand, the distinct groups recovered here may eventually be considered separate species. Adding more strains with a broader geographical range might reveal new, highly differentiated lineages. Multiple gene phylogenies and phylogenomic approaches that begin to emerge may result in better resolved divergence patterns (LaJeunesse et al. 2012, Orr et al. 2012). New analytical developments may reveal genetic differences that relate to reproductive isolation and might facilitate direct assessment of biological criteria for species boundaries. Comparisons of representatives from different ecological regimes at the genome and transcriptome level might highlight the importance of ecological criteria (Boenigk et al. 2012). Addressing reticulate evolution and hybridization might further support species delimitation. Differences in DNA contents that may indicate ploidy changes have been established for closely related dinoflagellate species and their potential in delimiting species has been emphasized although the approach needs further refinement (Figueroa et al. 2010). Future integrative taxonomic studies will show to what extent the species concept proposed here for *A. ostenfeldii* reflects a "separately evolving metapopulation lineage" sensu de Queiroz (2007).

We thank T. Alpermann, D. Anderson, I. Bravo, E. Bresnan, H. Gu, L. Percy, and N. Touzet for providing strains of *A. ostenfeldii/peruvianum*. H. Gudfinnson, V. Pospelova, B. Dale, and S. Sanchez collected sediment or water samples from Iceland, Canada, Norway, and Peru for new isolations. H. Kankaanpää, K. Harju, and W. Drebing contributed to the toxin analyses. Technical support was provided by J. Oja, M. Vandersea, and R. York. The advice of S. Nagai and P.T. Lim on molecular analyses and their interpretations are greatly appreciated. Steven Kibler and Christopher Holland provided helpful critical reviews of the manuscript. This work was supported by the Academy of Finland grant #128833 to AK and SS, the Maj and Tor Nessling Foundation (P.T.) and funding from the North Pacific Research Board Project 1021 (W.L.).

Aasen, J., MacKinnon, S. L., LeBlanc, P., Walter, J. A., Hovgaard, P., Aune, T. & Quilliam, M. A. 2005. Detection and identification of spirolides in Norwegian shellfish and plankton. *Chem. Res. Toxicol.* 18:509–15.

Adachi, M., Sako, Y. & Ishida, Y. 1994. Restriction fragment length polymorphism of ribosomal DNA internal transcribed spacer and 5.8S regions in Japanese *Alexandrium* species (Dinophyce- ae). *J. Phycol.* 30:857–63.

Amato, A., Kooistra, W., Ghiron, J. H. L., Mann, D. G., Pröschold, T. & Montresor, M. 2007. Reproductive isolation among sympatric cryptic species in marine diatoms. *Protist* 158:193–207.

Anderson, D. M., Alpermann, T. J., Cembella, A. D., Collos, Y., Masseret, E. & Montresor, M. 2012. The globally distributed genus *Alexandrium*: multifaceted roles in marine ecosystems and impacts on human health. *Harmful Algae* 14:10–35.

Balech, E. 1995. *The Genus* Alexandrium *Halim (Dinoflagellata)*. Sherkin Island Marine Station, Sherkin Island Co, Cork, Ireland, 151 pp.

Balech, E. & de Mendiola, B. R. 1977. Un nuevo *Gonyaulax* productor de hemotalasia en Peru. *Neotropica* 23:49–54.

Balech, E. & Tangen, K. 1985. Morphology and taxonomy of toxic species in the tamarensis group (Dinophyceae): *Alexandrium excavatum* (Braarud) comb. nov. and *Alexandrium ostenfeldii* (Paulsen) comb. nov. *Sarsia* 70:333–43.

Biecheler, B. 1952. Recherches sur les Peridinens. *Bull. Biol. France Belgique Suppl.* 36:1–149.

Boenigk, J., Ereshefsky, M., Hoef-Emden, K., Mallet, J. & Bass, D. 2012. Concepts in protistology: Species definitions and boundaries. *Eur. J. Protistol.* 48:96–102.

Bolch, C. J. S. & de Salas, M. F. 2007. A review of the molecular evidence for ballast water introduction of the toxic dinoflagellates *Gymnodinium catenatum* and the *Alexandrium tamarensis* complex to Australasia. *Harmful Algae* 6:465–85.

Borkman, D. G., Smayda, T. J., Tomas, C. R., York, R., Strangman, W. & Wrigh, J. L. C. 2012. *Alexandrium peruvianum* (Balech

and de Mendiola) Balech and Tangen in Narragansett Bay, Rhode Island (USA). *Harmful Algae* 19:92–100.

Bravo, I., Garces, E., Diogene, J., Fraga, S., Sampedro, N. & Figueroa, R. I. 2006. Resting cysts of the toxigenic dinoflagellate genus *Alexandrium* in recent sediments from the Western Mediterranean coast, including first description of cysts of *A. kutnerae* and *A. peruvianum*. *Eur. J. Phycol.* 41:293–302.

Brosnahan, M. L., Kulis, D. M., Solow, A. R., Erdner, D. L., Percy, L., Lewis, J. & Anderson, D. M. 2010. Outbreeding lethality between toxic group I and nontoxic Group III *Alexandrium tamarense* spp, isolates: predominance of heterotypic encystment and implications for mating interactions and biogeography. *Deep Sea Res. Part II: Topical Studies in Oceanography* 57:175–89.

Brown, L., Bresnan, E., Graham, J., Lacaze, J. P., Turrell, E. & Collins, C. 2010. Distribution, diversity and toxin composition of the genus *Alexandrium* (Dinophyceae) in Scottish waters. *Eur. J. Phycol.* 45:375–93.

Bryant, D. & Moulton, V. 2004. Neigbor-Net: an agglomerative method for the construction of phylogenetic networks. *Mol. Biol. Evol.* 21:255–65.

Cembella, A., Lewis, N. & Quilliam, M. 2000. The marine dinoflagellate *Alexandrium ostenfeldii* (Dinophyceae) as a causative organism of spirolide shellfish toxins. *Phycologia* 39:67–74.

Ciminiello, P., Dell'Aversano, C., Fattorusso, E., Magno, S., Tartaglione, L., Cangini, M., Pompei, M., Guerrini, F., Boni, L. & Pistocchi, R. 2006. Toxin profile of *Alexandrium ostenfeldii* (Dinophyceae) from the Northern Adriatic Sea revealed by liquid chromatography-mass spectrometry. *Toxicon* 47:597–604.

Coleman, A. 2009. Is there a molecular key to the level of "biological species" in eukaryotes? A DNA guide. *Mol. Phylogenet. Evol.* 50:197–203.

Darty, K., Denise, A. & Ponty, Y. 2009. VARNA: interactive drawing and editing of the RNA secondary structure. *Bioinformatics* 25:1974–5.

Diener, M., Erler, K., Hiller, S., Christian, B. & Luckas, B. 2006. Determination of Paralytic Shellfish Poisoning (PSP) toxins in dietary supplements by application of a new HPLC/FD method. *Eur. Food Res. Technol.* 224:147–51.

Figueroa, R. I., Bravo, I. & Garcés, E. 2008. The significance of sexual versus asexual cyst formation in the life cycle of the noxious dinoflagellate *Alexandrium peruvianum*. *Harmful Algae* 7:653–63.

Figueroa, R. I., Garces, E. & Bravo, I. 2010. The use of flow cytometry for species identification and life cycle studies in dinoflagellates. *Deep Sea Res. Part II: Topical Studies in Oceanography*. 57:301–7.

Franco, J. M., Paz, B., Riobo, P., Pizarro, G., Figueroa, R., Fraga, S., Bravo, I. 2006. *First Report of the Production of Spirolides by Alexandrium peruvianum* (Dinophyceae) from the Mediterranean Sea. Abstracts 12th International Conference on Harmful Algae, Copenhagen, Denmark, 397 pp.

Fritz, L. & Triemer, R. E. 1985. A rapid simple technique utilizing calcofluor white M2R for the visualization of dinoflagellate thecal plates. *Phyco. L.* 2:662–4.

Gouy, M., Guindon, S. & Gascuel, O. 2010. SeaView version 4: a multiplatform graphical user interface for sequence alignment and phylogenetic tree building. *Mol. Biol. Evol.* 27:221–4.

Gribble, K. E., Keafer, B. A., Quilliam, M. A., Cembella, A. D., Kulis, D. M., Manahan, A. & Anderson, D. M. 2005. Distribution and toxicity of *Alexandrium ostenfeldii* (Dinophyceae) in the Gulf of Maine, USA. *Deep-Sea Res. II* 52:2745–63.

Gu, H. 2011. Morphology, phylogenetic position, and ecophysiology of *Alexandrium ostenfeldii* (Dinophyceae) from the Bohai Sea, China. *J. Syst. Evol.* 49:606–16.

Guillard, R. R. L. & Ryther, J. H. 1962. Studies of marine planktonic diatoms. I. *Cyclotella nana* Hustedt and *Detonula confervacea* Cleve. *Can. J. Microbiol.* 8:229–39.

Hackett, J. D., Wisecaver, J. H., Brosnahan, M. L., Kulis, D. M., Anderson, D. M., Bhattacharya, D., Plumley, F. G. & Erdner, D. L. 2013. Evolution of saxitoxin synthesis in cyanobacteria and dinoflagellates. *Mol. Biol. Evol.* 30:70–8.

Hakanen, P., Suikkanen, S., Franzén, J., Franzén, H., Kankaanpää, H. & Kremp, A. 2012. Bloom and toxin dynamics of *Alexandrium ostenfeldii* in a shallow embayment at the SW coast of Finland, northern Baltic Sea. *Harmful Algae* 15:91–9.

Hansen, P. J., Cembella, A. D. & Moestrup, Ø. 1992. The marine dinoflagellate *Alexandrium ostenfeldii*: paralytic shellfish toxin concentration, composition, and toxicity to a tintinnid ciliate. *J. Phycol.* 28:597–603.

Hansen, G., Daugbjerg, N. & Franco, J. M. 2003. Morphology, toxin composition and LSU rDNA phylogeny of *Alexandrium minutum* (Dinophyceae) from Denmark, with some morphological observations on other European strains. *Harmful Algae* 2:317–35.

Hsia, M. H., Morton, S. L., Smith, L. L., Beauchesne, K. R., Huncik, K. M. & Moeller, P. D. R. 2006. Production of goniodomin A by the planktonic, chain-forming dinoflagellate *Alexandrium monilatum* (Howell) Balech isolated from the Gulf coast of the United States. *Harmful Algae* 5:290–9.

Huson, D. H. & Bryant, D. 2006. Application of phylogenetic networks in evolutionary studies. *Mol. Biol. Evol.* 23:254–67.

Janiszewski, J. & Boyer, G. L. 1993. The electrochemical oxidation of saxitoxin and derivatives: its application to the HPLC of PSP toxins. *In* Smayda, T. J. & Shimizu, Y. [Eds.] *Toxic Phytoplankton Blooms in the Sea*. Elsevier, New York, pp. 889–94.

John, U., Fensome, R. A. & Medlin, L. K. 2003. The application of a molecular clock based on molecular sequences and the fossil record to explain biogeographic distributions within the *Alexandrium tamarense* "species complex" (Dinophyceae). *Mol. Biol. Evol.* 20:1015–27.

Katoh, K., Asimenos, G. & Toh, H. 2009. Multiple alignment of DNA sequences with MAFFT. *Method. Mol. Biol.* 537:39–64.

Koetschan, C., Förster, F., Keller, A., Schleicher, T., Ruderisch, B., Schwarz, R., Müller, T., Wolf, M. & Schultz, J. 2010. The ITS2 Database III - sequences and structures for phylogeny. *Nucleic Acids Res.* 38:D275–9.

Kremp, A. 2013. Diversity of dinoflagellate life cycles: facets and implications of complex strategies. *In* Lewis, J. M., Marret, F. & Bradlay, L. [Eds.] *Biological and Geological Perspectives of Dinoflagellates*. The Micropalaeontological Society, Special Publications, Geological Society, London, pp. 189–98.

Kremp, A., Lindholm, T., Dreßler, N., Erler, K., Gerdts, G., Eirtovaara, S. & Leskinen, E. 2009. Bloom forming *Alexandrium ostenfeldii* (Dinophyceae) in shallow waters of the Åland Archipelago, Northern Baltic Sea. *Harmful Algae* 8:318–28.

Krock, B., Seguel, C. G. & Cembella, A. D. 2007. Toxin profile of *Alexandrium catenella* from the Chilean coast as determined by liquid chromatography with fluorescence detection and liquid chromatography coupled with tandem mass spectrometry. *Harmful Algae* 6:734–44.

LaJeunesse, T. C., Parkinson, J. E. & Reimer, J. D. 2012. A genetics-based description of *Symbiodinium minutum* sp. nov. and *S. psygmophilum* sp. nov. (Dinophyceae), two dinoflagellates symbiotic with cnidaria. *J. Phycol.* 48:1380–91.

Leaw, C. P., Lim, P. T., Ng, B. K., Cheah, M. Y., Ahmad, A. & Usup, G. 2005. Phylogenetic analysis of *Alexandrium* species and *Pyrodinium bahamense* (Dinophyceae) based on theca morphology and nuclear ribosomal gene sequence. *Phycologia* 44:550–65.

Leaw, C. P., Lim, P. T., Ng, B. K., Cheng, K. W. & Usup, G. 2010. Morphology and molecular characterization of a new species of thecate benthic epiphytic dinoflagellate, *Coolia malayensis* sp. nov. (Dinophyceae). *J. Phycol.* 46:162–71.

Lilly, E. L., Halanych, K. M. & Anderson, D. M. 2005. Phylogeny biogeography and species boundaries within the *Alexandrium minutum* group. *Harmful Algae* 4:1004–20.

Lilly, E. L., Halanych, K. M. & Anderson, D. M. 2007. Species boundaries and global biogeography of the *Alexandrium tamarense* complex (Dinophyceae). *J. Phycol.* 43:1329–38.

Lim, P. T., Usup, G., Leaw, C. P. & Ogata, T. 2005. First report of *Alexandrium taylori* and *Alexandrium peruvianum* (Dinophyceae) in Malaysia waters. *Harmful Algae* 4:391–400.

Litaker, R. W., Vandersea, M. W., Kibler, S. R., Reece, K. S., Stokes, N. A., Lutzoni, F. M., Yonish, B. A., West, M. A., Black, M. N. D. & Tester, P. A. 2007. Recognizing dinoflagellate species using ITS rDNA sequences. *J. Phycol.* 43:344–55.

MacKenzie, L., de Salas, M., Adamson, J. & Beuzenberg, V. 2004. The dinoflagellate genus *Alexandrium* (Halim) in New Zealand coastal waters: comparative morphology, toxicity and molecular genetics. *Harmful Algae* 3:71–92.

MacKenzie, L., White, D., Oshima, Y. & Kapa, J. 1996. The resting cyst and toxicity of *Alexandrium ostenfeldii* (Dinophyceae) in New Zealand. *Phycologia* 35:148–55.

MacLean, C., Cembella, A. D. & Quilliam, M. A. 2003. Effects of light, salinity and inorganic nitrogen on cell growth and spirolide production in the marine dinoflagellate *Alexandrium ostenfeldii* (Paulsen) Balech et Tangen. *Bot. Mar.* 46:466–76.

Martins, C. A., Kulis, D., Franca, S. & Anderson, D. M. 2004. The loss of PSP toxin production in a formerly toxic *Alexandrium lusitanicum* clone. *Toxicon* 43:195–205.

Mathews, D. H. 2004. Using an RNA secondary structure partition function to determine confidence in base pairs predicted by free energy minimization. *RNA* 10:1178–90.

Mayr, E. 1942. *Systematics and the Origin of Species*. Columbia University Press, New York.

McCauley, L. A. R., Erdner, D. L., Nagai, S., Richlen, M. L. & Anderson, D. M. 2009. Biogeographic analysis of the globally distributed harmful algal bloom species *Alexandrium minutum* (Dinophyceae) based on rRNA gene sequences and microsatellite markers. *J. Phycol.* 45:454–63.

Miranda, L. N., Zhuang, Y., Zhang, H. & Lin, S. 2012. Phylogenetic analysis guided by intragenomic SSU rDNA polymorphism refines classification of ''*Alexandrium tamarense*'' species complex. *Harmful Algae* 16:35–48.

Nagai, S., Baba, B., Miyazono, A., Tahvanainen, P., Kremp, A., Godhe, A., MacKenzie, L. & Anderson, D. M. 2010. Polymorphisms of the nuclear ribosomal RNA genes found in the different geographic origins in the toxic dinoflagellate *Alexandrium ostenfeldii* and the species detection from a single cell by LAMP. *DNA Polymorphism* 18:122–6.

Orr, R. J. S., Murray, S. A., Stüken, A., Rhodes, L. & Jakobsen, K. S. 2012. When naked became armored: an eight-gene phylogeny reveals monophyletic origin of theca in Dinoflagellates. *PLoS ONE* 7:e50004.Doi: 10.1371/journal.pone.0050004.

Orr, R. J. S., Stüken, A., Rundberget, T., Eikrem, W. & Jakobsen, K. S. 2011. Improved phylogenetic resolution of toxic and non-toxic *Alexandrium* strains using a concatenated rDNA approach. *Harmful Algae* 10:676–88.

Østergaard-Jensen, M. & Moestrup, Ø. 1997. Autoecology of the toxic dinoflagellate *Alexandrium ostenfeldii*: life history and growth at different temperatures and salinities. *Eur. J. Phycol.* 32:9–18.

Paulsen, O. 1904. Plankton investigations in the waters round Island in 1903. *Meddelser fra Komm. Havunders. Se. Plank.* 1:1–40.

Penna, A., Garcés, E., Vila, M., Giacobbe, M. G., Fraga, S., Lugliè, A., Bravo, I., Bertozzini, E. & Vernesi, C. 2005. *Alexandrium catenella* (Dinophyceae), a toxic ribotype expanding in the NW Mediterranean Sea. *Mar. Biol.* 148:13–23.

Percy, L., Morris, S., Higman, W., Stone, D., Hardstaff, W. R., Quilliam, M. A. & Lewis, J. 2004. Identification of *Alexandrium ostenfeldii* from the Fal Estuary, UK; morphology, molecular taxonomy and toxin composition. Abstract, XI International Conference on Harmful Algal Blooms, Cape Town, South Africa, 15–19 November, 2004, 209 pp.

Pfiester, L. A. & Anderson, D. M. 1987. Dinoflagellate reproduction. *In* Taylor, F.J.R.[Ed.] *The Biology of Dinoflagellates*. Blackwell Scientific Publications, Oxford, pp.611–648.

Posada, D. 2008. jModelTest: phylogenetic model averaging. *Mol. Biol. Evol.* 25:1253–6.

Pritchard, J. K., Stephens, M. & Donnelly, P. 2000. Inference of population structure using multilocus genotype data. *Genetics* 155:945–59.

de Queiroz, K. 2007. Species concepts and species delimitation. *Syst. Biol.* 56:879–86.

Quijano-Scheggia, S. I., Garces, E., Lundholm, N., Moestrup, Ø., Andree, K. & Camp, J. 2009. Morphology, physiology, molecular phylogeny and sexual compatibility of the cryptic *Pseudo-nitzschia delicatissima* complex (Bacillariophyta), including the description of *P. arenyensis* sp. nov. *Phycologia* 48:492–509.

Rambaut, A. & Drummond, A. J. 2007. Tracer v1.4, BEAST Software website. Available at: http://beast.bio.ed.ac.uk/Tracer (accessed August 5, 2011).

Rodríguez, F., Oliver, J. L., Marín, A. & Medina, J. R. 1990. The general stochastic model of nucleotide substitution. *J. Theor. Biol.* 142:485–501.

Ronquist, F. & Huelsenbeck, J. P. 2003. MRBAYES 3: Bayesian phylogenetic inference under mixed models. *Bioinformatics* 19:1572–4.

Sanchez, S., Villanueva, P. & Carbajo, L. 2004. Distribution and concentration of *Alexandrium peruvianum* (Balech and de Mendiola) in the Peruvian coast (03°24′–18°20′ LS) between 1982–2004. Abstracts, XI International Conference on Harmful Algal Blooms, Cape Town, South Africa, November 15–19, 2004, 227 pp.

Scholin, C. A., Herzog, M., Sogin, M. & Anderson, D. M. 1994. Identification of group- and strain-specific genetic markers for globally distributed *Alexandrium* (Dinophyceae). II. Sequence analysis of a fragment of the LSU rRNA gene. *J. Phycol.* 30:999–1011.

Smith, C., Heyne, S., Richter, A. S., Will, S. & Backofen, R. 2010. Freiburg RNA Tools: a web server integrating IntaRNA, ExpaRNA and LocARNA. *Nucl. Acids Res.* 38(Suppl. 2): W373–7. Doi: 10.1093/nar/gkq316.

Stüken, A., Orr, R. J. S., Kellmann, R., Murray, S. A., Neilan, B. A. & Jakobsen, K. S. 2011. Discovery of nuclear-encoded genes for the neurotoxin saxitoxin in dinoflagellates. *PLoS ONE* 6: e20096.

Suikkanen, S., Kremp, A., Hautala, H. & Krock, B. 2013. Paralytic Shellfish Toxins or Spirolides? The role of environmental and genetic factors in toxin production of *Alexandrium ostenfeldii/peruvianum*. *Harmful Algae* 26:52–9.

Swofford, D. L. 2003. *PAUP*. Phylogenetic Analysis Using Parsimony (*and Other Methods)* [Version 4.] Sinauer Associates, Sunderland, Massachusetts.

Tahvanainen, P., Alpermann, T. J., Figueroa, R. I., John, U., Hakanen, P., Nagai, S., Blomster, J. & Kremp, A. 2012. Patterns of post-glacial genetic differentiation in marginal populations of a marine micro-alga. *PLoS ONE* 7:e53602.

Taylor, F. J. R., Fukuyo, Y. & Larsen, J. 1995. Taxonomy of harmful dinoflagellates. *In* Hallegraeff, G. M., Anderson, D. M. & Cembella, A. D. [Eds.] *Manual on Harmful Marine Microalgae. IOC Manuals and Guides No. 33*. Intergovernmental Oceanographic Commission of UNESCO, Paris, pp. 33–42.

Tomas, C. R., van Wagoner, R., Tatters, A. O., Hall, S., White, K. & Wright, J. L. C. 2012. *Alexandrium peruvianum* (Balech and Mendiola) Balech and Tangen a new toxic species for coastal North Carolina. *Harmful Algae* 17:54–63.

Touzet, N., Franco, J. M. & Raine, R. 2008. Morphogenetic diversity and biotoxin composition of *Alexandrium* (Dinophyceae) in Irish coastal waters. *Harmful Algae* 7:782–97.

Touzet, N., Lacaze, J. P., Maher, M., Turrell, E. & Raine, R. 2011. Summerdynamics of *Alexandrium ostenfeldii* (Dinophyceae) and spirolide toxins in Cork Harbour, Ireland. *Mar. Ecol. Prog. Ser.* 425:21–33.

Van Wagoner, R. M., Misner, I., Tomas, C. R. & Wright, J. L. C. 2011. Occurrence of 12 methylgymnodimine in a spirolide-producing dinoflagellate *Alexandrium peruvianum* and the biogenic implications. *Tetrahedron Lett.* 52:4243–6.

Wang, D. Z. 2008. Neurotoxins from marine dinoflagellates: a brief review. *Mar. Drugs* 6:349–71.

Witek, B. 2004. Blooms of potential toxic dinoflagellates *Prorocentrum minimum* (Pavillard) and Schiller and *Alexandrium ostenfeldii* (Paulsen) Balech Tangen in the Gulf of Gdansk. Abstract: Ogolnopolska Konferencja Naukowa "Zakwity wody-monitoring i kontrola zagrozen", Gdynia 20–22 kwietnia 2004.

Zuker, M. 2003. Mfold web server for nucleic acid folding and hybridization prediction. *Nucleic Acids Res.* 31:3406–15.

Zwickl, D. J. 2006. Genetic algorithm approaches for the phylogenetic analysis of large biological sequence datasets under the maximum likelihood criterion. PhD dissertation, University of Texas, Austin, Texas.

Supporting Information

Additional Supporting Information may be found in the online version of this article at the publisher's web site:

Table S1. Unique LSU D1-D2 sequences included in the phylogenetic analysis presented in Figure 2.

Table S2. Cell size: Ranges and means (±SD) of length, width and length/width ratios of cells of *Alexandruim ostenfeldii* strains from different phylogenetic clades.